

Journal Pre-proof

Discovery of 3-(((9*H*-purin-6-yl)amino)methyl)-4,6-dimethylpyridin-2(1*H*)-one derivatives as novel tubulin polymerization inhibitors for treatment of cancer

Qiangsheng Zhang, Xi Hu, Guoquan Wan, Jia Wang, Lu Li, Xiuli Wu, Zhihao Liu, Luoting Yu



PII: S0223-5234(19)30880-3

DOI: <https://doi.org/10.1016/j.ejmech.2019.111728>

Reference: EJMECH 111728

To appear in: *European Journal of Medicinal Chemistry*

Received Date: 5 August 2019

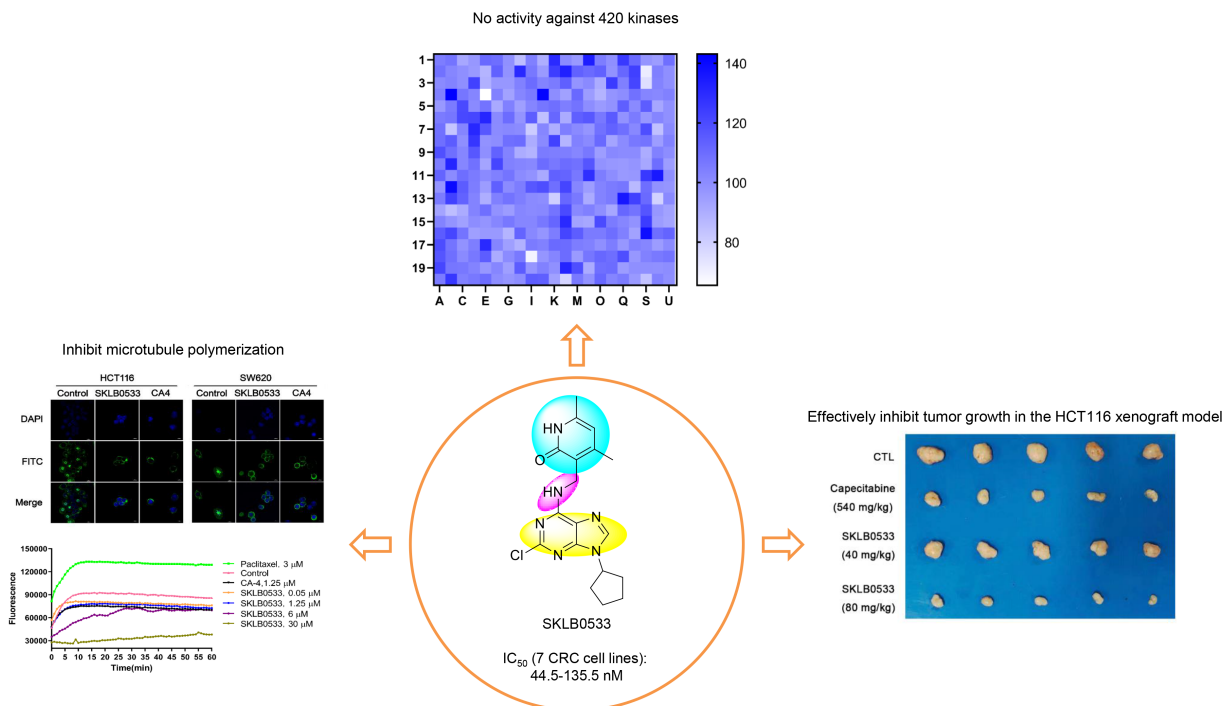
Revised Date: 20 September 2019

Accepted Date: 21 September 2019

Please cite this article as: Q. Zhang, X. Hu, G. Wan, J. Wang, L. Li, X. Wu, Z. Liu, L. Yu, Discovery of 3-(((9*H*-purin-6-yl)amino)methyl)-4,6-dimethylpyridin-2(1*H*)-one derivatives as novel tubulin polymerization inhibitors for treatment of cancer, *European Journal of Medicinal Chemistry* (2019), doi: <https://doi.org/10.1016/j.ejmech.2019.111728>.

This is a PDF file of an article that has undergone enhancements after acceptance, such as the addition of a cover page and metadata, and formatting for readability, but it is not yet the definitive version of record. This version will undergo additional copyediting, typesetting and review before it is published in its final form, but we are providing this version to give early visibility of the article. Please note that, during the production process, errors may be discovered which could affect the content, and all legal disclaimers that apply to the journal pertain.

© 2019 Published by Elsevier Masson SAS.



Discovery of 3-(((9*H*-purin-6-yl)amino)methyl)-4,6-dimethylpyridin-2(1*H*)-one derivatives as novel tubulin polymerization inhibitors for treatment of cancer

Qiangsheng Zhang^{a1}, Xi Hu^{a1}, Guoquan Wan^a, Jia Wang^a, Lu Li^a, Xiuli Wu^a, Zhihao Liu^{a*}, Luoting Yu^{a*}

^aState Key Laboratory of Biotherapy and Cancer Center, West China Hospital, West China Medical School, Sichuan University, and Collaborative Innovation Center for Biotherapy, 17#3rd Section, Ren Min South Road, Chengdu 610041, China.

¹These authors contribute equally to this work.

*Corresponding authors. Address: Lab of Medicinal Chemistry, State Key Laboratory of Biotherapy and Cancer Center, West China Hospital, Sichuan University and Collaborative Innovation Center for Biotherapy, 17#3rd Section, Ren Min South Road, Chengdu 610041, China. Phone: +86-28-85503817; Fax: +86-28-85164060. E-mail address: yuluot@scu.edu.cn (L.-T. Yu) & liuzhihao@scu.edu.cn (Z.-H. Liu)

Abstract:

A new series of 3-(((9*H*-purin-6-yl)amino)methyl)-4,6-dimethylpyridin-2(1*H*)-one derivatives were designed, synthesized and demonstrated to act as tubulin polymerization inhibitors. These new derivatives showed significant antitumor activities, among which SKLB0533 demonstrated to be the most potent compound, with IC₅₀ values ranging from 44.5 and 135.5 nM against seven colorectal carcinoma (CRC) cell lines. Remarkably, SKLB0533 exhibited no activity against other potential

targets, such as 420 kinases and EZH2. Besides, SKLB0533 inhibited tubulin polymerization, arrested the cell cycle at the G2/M phase and induced apoptosis in CRC cells. Furthermore, SKLB0533 suppressed tumour growth in the HCT116 xenograft model without inducing notable major organ-related toxicity, suggesting that SKLB0533 could be used as a promising lead compound for the development of new antitumor agents.

Keywords: Microtubule, Tubulin polymerization inhibitors, Anti-cancer agents, Colorectal carcinoma

1. Introduction

Morbidity and mortality due to cancer are growing rapidly worldwide, and cancer has become a serious public health problem. Estimates from the of 2018 global cancer report indicate that CRC is the third most common causes of cancer death worldwide in both males and females [1]. More than 1.5 million men and women living in the United States are estimated to have a previous colorectal cancer diagnosis, and 145,600 new cases will be diagnosed in 2019[2]. Moreover, an increasing number of young people are dying from CRC[3].

Microtubules (MTs) are dynamic filamentous cytoskeletal polymers of tubulin, which involved in numerous essential cellular functions, such as cell growth, division, motility and intracellular trafficking[4-6]. Disruption of microtubule dynamics increases the number of cells in metaphase arrest and mitotic catastrophe, which closely associated with the progression of cancer, including CRC [7, 8]. Due to the

important role of microtubules, especially in mitosis, they have become an important target for the design of new anticancer agents[9-11].

Today, microtubule-targeted drugs span a wide structural heterogeneity and contain several potent natural and synthetic compounds, such as Paclitaxel[12], Epothilone D[13], Laulimalide[14], Vincristine[15], Rhizoxin[16] and Colchicine[17]. Recently, a variety of colchicine binding site tubulin inhibitors containing a trimethoxyphenyl (TMP) moiety were designed for the treatment of cancer, such as Combretastatin A-4 (CA-4)[18], Ombrabulin[19] and Compound **8c4**[20] (**Fig. 1**).

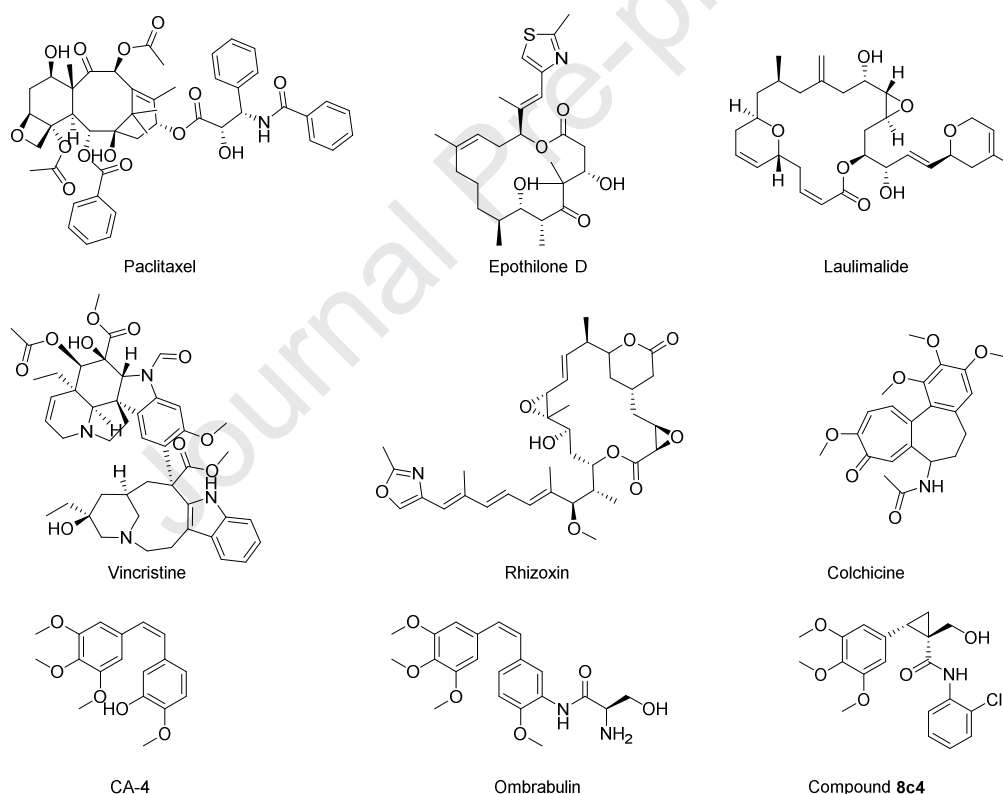


Fig. 1 Representative microtubule stabilizing and destabilizing agents.

Despite the advances have been undoubtedly made in microtubule-targeted agents, existing agents suffer from some significant drawbacks[21], such as limited effectiveness which can lead to treatment failure, drug resistance and adverse

toxicities can be dose-limiting, indicating a narrow therapeutic window [22]. Collectively, these shortcomings have encouraged medicinal chemists to develop novel antimitotic agents for cancer therapy[23-25].

Among the reported microtubule inhibitors, compounds owning concise double-ring core structure attracted our interest, such as MPC-6827[26], Compound **30** • HCl[27], Myoseverin[28] and E2GG[29]. By investigating these compounds, we found that such microtubule inhibitors were mainly composed of three parts (**Fig. 2**): the core structure (yellow box), which serves as skeletal support; the aromatic ring (blue box), which may participate in a π - π stacking with the amino acid residues around the binding site[30]; and the linker (purple box), which connects the core structure to the aromatic ring.

Based on the above findings, we chose purine as the core structure, aminomethyl as the linker firstly. Then, we replaced the aromatic ring with pyridin-2(1*H*)-one using a bioelectronic isosteric strategy. From the co-crystal structure of Colchicine bound to the tubulin (PDB code: 4O2B), we could see that trimethoxyphenyl motif surrounded by residues Cys β 241, Leu β 248, Asn β 249, Ala β 250, Asp β 251 and Lys β 254. So compared to the phenyl ring, pyridin-2(1*H*)-one retained aromaticity and contained a hydrogen bond acceptor and hydrogen bond donor, which may increase its hydrogen bonding interactions[31]. Herein, a series of 3-(((9*H*-purin-6-yl)amino)methyl)-4,6-dimethylpyridin-2(1*H*)-one derivatives were designed.

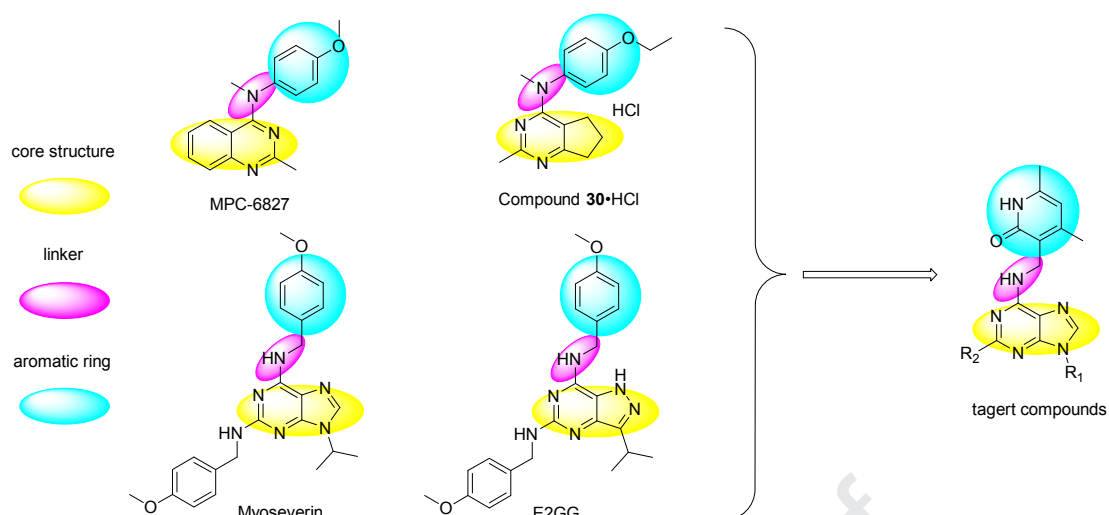


Fig. 2 Rational design of new tubulin-targeted compounds.

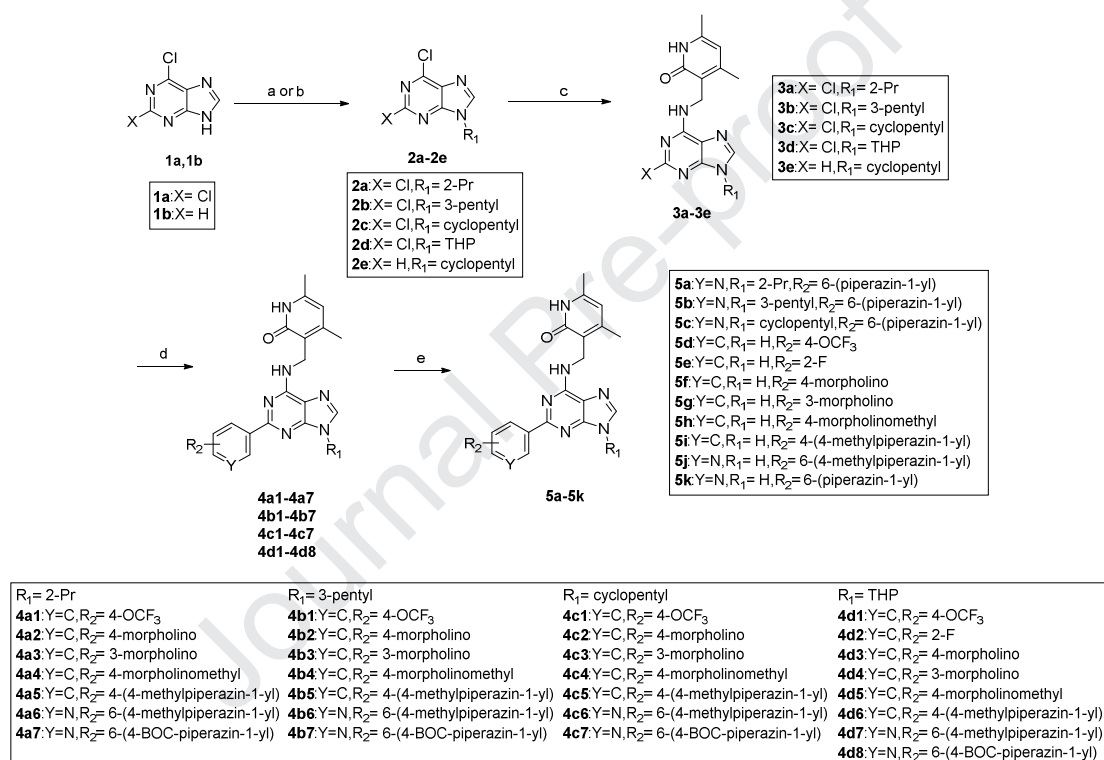
2. Results and discussion

2.1. Chemistry

3-(((9*H*-purin-6-yl)amino)methyl)-4,6-dimethylpyridin-2(1*H*)-one derivatives were synthesized by a two-four step procedure summarized in **Scheme 1**. Compounds **3a-3d** were synthesized from commercially available 2,6-dichloro-1*H*-purine in two steps: (1) 2,6-dichloro-1*H*-purine was reacted with halogenated alkane under basic conditions to give compounds **2a-2c**[32]. Compound **2d** was obtained by protecting the amino group with tetrahydropyran (THP) under *p*-toluenesulfonic acid (*p*-TsOH). (2) Compounds **3a-3d** were synthesized in high yields by reacting compounds **2a-2d** with 3-(aminomethyl)-4,6-dimethylpyridin-2(1*H*)-one[33]. Compounds **4a1-4d8** were obtained using the Suzuki-Miyaura reaction by coupling them to corresponding boric acid or borate derivatives in a 1,1'-bis(diphenylphosphino) ferrocene catalytic system in the presence of sodium carbonate (Na₂CO₃) as the base in dioxane/water at 100 °C for 4 h. Finally, compounds **4a7**, **4b7**, **4c7** and **4d1-4d8** were stirred at room

temperature overnight with trifluoroacetic acid (TFA) to remove the THP or tert-butyloxycarbonyl (Boc) protecting group and obtain the target compounds **5a-5k**.

The structures of 3-(((9*H*-purin-6-yl)amino)methyl)-4,6-dimethylpyridin-2(1*H*)-one derivatives were confirmed by NMR (^1H & ^{13}C) and HRMS spectral analyses. The purity of all the newly synthesized compounds was more than 98% as analysed by HPLC.



Scheme 1 Synthesis of the target compounds. (a) Halogenated alkane, K_2CO_3 , anhydrous DMSO, 150 °C, overnight. (b) 3,4-Dihydro-2*H*-pyran, *p*-TsOH, DCM, r.t., 8 h. (c) 3-(aminomethyl)-4,6-dimethylpyridin-2(1*H*)-one, EtOH, 80 °C, 6 h. (d) Boric acid or borate derivatives, $\text{PdCl}_2(\text{dppf}) \cdot \text{CH}_2\text{Cl}_2$, Na_2CO_3 , dioxane/water, 100 °C, 4 h. (e) TFA, DCM, r.t., overnight.

2.2. Structure -activity relationships

All the 3-(((9*H*-purin-6-yl)amino)methyl)-4,6-dimethylpyridin-2(1*H*)-one

derivatives were evaluated to the antiproliferative activity against three cancer cell lines HepG2 (hepatocellular carcinoma cells), HCT116 (colorectal carcinoma cells) and A549 (lung cancer cells) using the MTT assay in terms of half maximal inhibitory concentration (IC₅₀) values. For comparison, Myoseverin and CA-4 were selected as the positive references (**Tab. 1**).

Generally, most of the synthesized compounds inhibited the growth of the three cancer cells lines, with IC₅₀ values less than 5 μ M. Approximately one-third of tested compounds were superior to Myoseverin with IC₅₀ values less than 1 μ M.

The 2-Pr,3-pentyl or cyclopentyl substituents on the N9-position of the purine derivatives (**3a-3d**, **4a1-4a7**, **4b1-4b7** and **4c1-4c7**) provided increased antiproliferative activity. The antiproliferative activity was significantly reduced if the 2-Pr,3-pentyl or cyclopentyl substituents were absent at position 1 (as in **5a-5k** compared to **3a-3d**, **4a1-4a7**, **4b1-4b7** and **4c1-4c7**) or if the substituent at position 1 was a tetrahydropiran instead of 2-Pr,3-pentyl or cyclopentyl (compare **4d1-4d8** versus **3a-3d**, **4a1-4a7**, **4b1-4b7** and **4c1-4c7**). These results suggested that suitable alkyl substituents at the N9-position may be advantageous.

Comparison of compounds **3a-3d** with other compounds revealed that a 2-chloro substitution on the purine ring led to a remarkable improvement in antiproliferative activity. The antiproliferative activity of the synthesized compounds with different substituents at position 2 increased in the following order: **3a-3d** (chloro) > **4a1**, **4b1**, **4c1** (4-(trifluoromethoxy)phenyl) > **4a2-4a4**, **4b2-4b4**, **4c2-4c4** (4-morpholinophenyl, 3-morpholinophenyl, 4-(morpholinomethyl)phenyl) > **4a5-4a7**, **4b5-4b7**, **4c5-4c7**

(4-(4-methylpiperazin-1-yl)phenyl, 6-(4-methylpiperazin-1-yl)pyridin-3-yl, 6-(4-Boc-piperazin-1-yl)pyridin-3-yl). Compared **3c** (SKLB0533) with compound **3a**, **3b**, **3d** and **3e**, we hypothesize that different substituents at the N9 position may affect the interaction of C6 chlorine and surrounding residues. SKLB0533 could inhibit the polymerization of tubulin more effectively. By comparing the antiproliferative activity of a C2-position hydrogen substitution, chlorine substitution and benzene ring substitution, we can speculate that the suitable size substituent group at the C2-position may be beneficial.

In this study, we did not examine the effect of different pyridin-2(1*H*)-one substitutions on antiproliferative activity, which will be the focus of our next stage of work.

Notably, SKLB0533 exhibited the most potent antiproliferative activity among the synthesized compounds, with IC_{50} values ranging between 0.06 and 0.10 μ M. SKLB0533 was more active against the three tested cancer cell lines than Myoseverin (3.06 to >10 μ M). Meanwhile SKLB0533 was 10- to 20-fold less active than CA-4 against the HpeG2 and A549 cell lines, which was superior to CA-4 against the HCT116 cell lines in our test.

Tab. 1 Antiproliferative activities of the target compounds.

Cpd.	IC ₅₀ /μM			Cpd.	IC ₅₀ /μM		
	HepG2	HCT116	A549		HepG2	HCT116	A549
3a	0.15±0.01	1.86±0.33	1.13±0.05	4c6	7.63±0.84	>10	5.17±0.06
3b	0.20±0.06	1.33±0.26	1.51±0.06	4c7	1.62±0.00	1.01±0.00	>10
3c (SKLB 0533)	0.08±0.01	0.06±0.00	0.10±0.01	4d1	5.22±0.08	5.83±0.06	9.46±0.04
3d	0.41±0.01	2.71±0.13	1.93±0.27	4d2	>10	>10	>10
3e	/	1.05±0.23	>10	4d3	>10	>10	>10
4a1	2.47±0.07	0.55±0.08	9.31±0.01	4d4	6.67±0.19	8.27±0.27	>10
4a2	1.11±0.07	1.03±0.08	4.30±0.28	4d5	>10	>10	>10
4a3	>10	7.42±0.54	>10	4d6	>10	>10	>10
4a4	0.93±0.02	8.01±0.36	>10	4d7	>10	9.05±0.00	>10
4a5	5.81±0.14	7.93±0.75	4.72±0.12	4d8	>10	9.07±0.04	>10
4a6	>10	8.99±0.03	>10	5a	2.88±0.22	1.19±0.05	>10
4a7	>10	4.14±0.36	0.49±0.01	5b	5.72±0.00	3.94±0.03	6.13±0.02
4b1	1.42±0.13	0.78±0.02	5.38±0.30	5c	1.71±0.10	0.85±0.08	>10
4b2	1.54±0.030	>10	5.90±0.05	5d	1.29±0.09	1.08±0.01	>10
4b3	2.22±0.16	>10	>10	5e	6.89±0.06	6.91±0.19	>10
4b4	1.82±0.01	2.99±0.01	6.13±0.12	5f	4.74±0.01	5.66±0.31	>10
4b5	1.99±0.09	>10	5.09±0.02	5g	5.19±0.63	6.84±1.34	>10
4b6	0.82±0.10	0.65±0.23	>10	5h	>10	>10	>10
4b7	0.52±0.13	0.88±0.07	8.21±0.11	5i	9.83±0.87	>10	>10
4c1	6.21±0.41	7.55±0.78	>10	5j	>10	>10	>10
4c2	0.98±0.05	0.52±0.04	>10	5k	6.02±0.07	2.65±0.10	>10
4c3	0.89±0.020	5.32±0.19	2.65±0.19	Myosev- erin CA-4 (nM)	3.06±0.31	7.82±0.17	>10
4c4	1.93±0.07	2.46±0.20	>10		3±2	212±0	7±0
4c5	2.59±0.30	1.37±0.18	6.21±0.01				

Data are expressed as the mean \pm SEM for at least 2 independent experiments.

2.3. Effect on tubulin polymerization

Since the vital role of tubulin-microtubule system in the maintenance of cellular morphology and basic cellular functions, we examined the effect of SKLB0533 on the organization of the microtubule network in living cells. Based on the obtained IC₅₀ values against the three cancer cell lines, SKLB0533 was evaluated for cell-based immunofluorescence staining assays at 50 nM. As shown in **Fig. 3A**, cells without drug treatment (control group) maintained a well-organized spindle and microtubule network. However, after cells were treated with SKLB0533 for 18 h, the microtubule network became disorganized and condensed around the nucleus, similar to the disruption produced by CA-4 at the same concentration. These results confirm that SKLB0533 is able to disrupt the microtubule network at low concentrations in HCT116 and SW620 cells.

An *in vitro* tubulin polymerization assay was used to prove the impact of SKLB0533 on the tubulin polymerization dynamics, CA-4 was used as a positive control and paclitaxel was utilized as a negative control. As illustrated in **Fig. 3B**, paclitaxel immediately and obviously increased the absorbance, indicating that this compound enhanced tubulin polymerization. By contrast, CA-4 and SKLB0533 decreased the absorbance, indicating that tubulin polymerization was inhibited. Meanwhile, low concentration of SKLB0533 (0.05 μ M) could inhibit microtubule polymerization. The microtubule inhibition was enhanced with the increased concentration of SKLB0355, which showed strong inhibition at 30 μ M. These results

clearly indicate that SKLB0533 significantly inhibits the polymerization of tubulin *in vitro*.

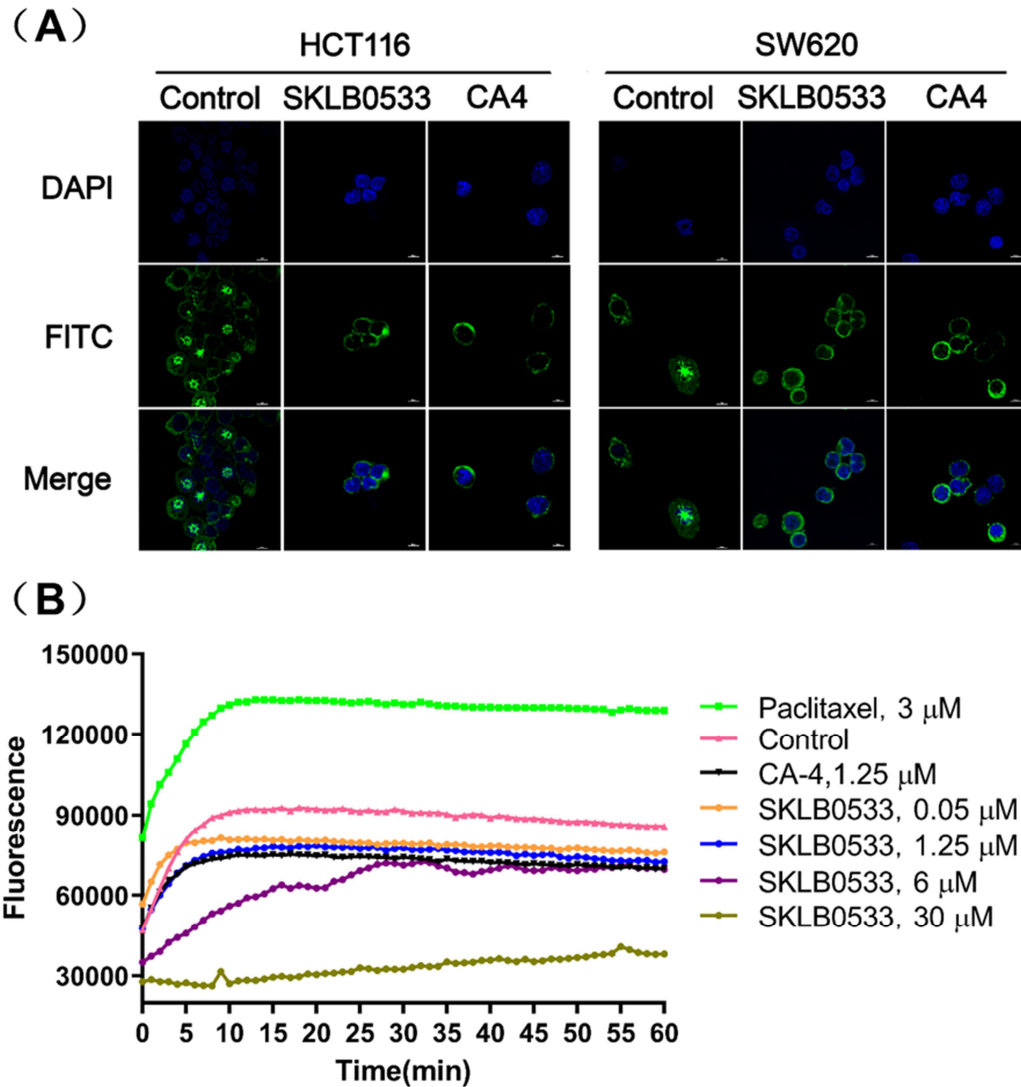


Fig. 3 Effects of SKLB0533 on tubulin polymerization *in vitro*. (A) Effect of 50 nM SKLB0533 on the organization of the microtubule network. HCT116 and SW620 cells were treated with 50 nM SKLB0533 for 18 h. Control was treated with 0.1% DMSO. Tubulin labelled with a monoclonal β -tubulin antibody (green) and nuclei labelled with DAPI (blue) were observed under a confocal fluorescence microscope (scale bar = 10 μ m). (B) Polymerization of tubulin at 37 $^{\circ}$ C in the presence of

paclitaxel (3 μ M), CA-4 (1.25 μ M), and SKLB0533 (0.05, 1.25, 6 and 30 μ M).

2.4. Molecular modeling

To investigate the possible binding mode for this series of compounds, the most potent compound SKLB0533 was docked into the tubulin-Colchicine complex (PDB code: 4O2B). As shown in **Fig. 4**, SKLB0533 was bound in the same location as the Colchicine, with the purine-aminomethyl-pyridone located towards the β -subunit and surrounded by residues Cys β 241, Leu β 248, Asn β 249, Ala β 250, Asp β 251, Lys β 254, Leu β 255, Asn β 258, Met β 259, Thr β 314, Val β 315, Ala β 316, Thr β 353 and Ala β 354. There was hydrogen bond between the ketone of pyridin-2(1*H*)-one fragment and the NH of Asp β 251. And the N7 of purine ring formed a hydrogen interaction with the NH of Asp β 258. Besides the hydrogen interactions, there were some hydrophobic interactions with the surrounding residues.

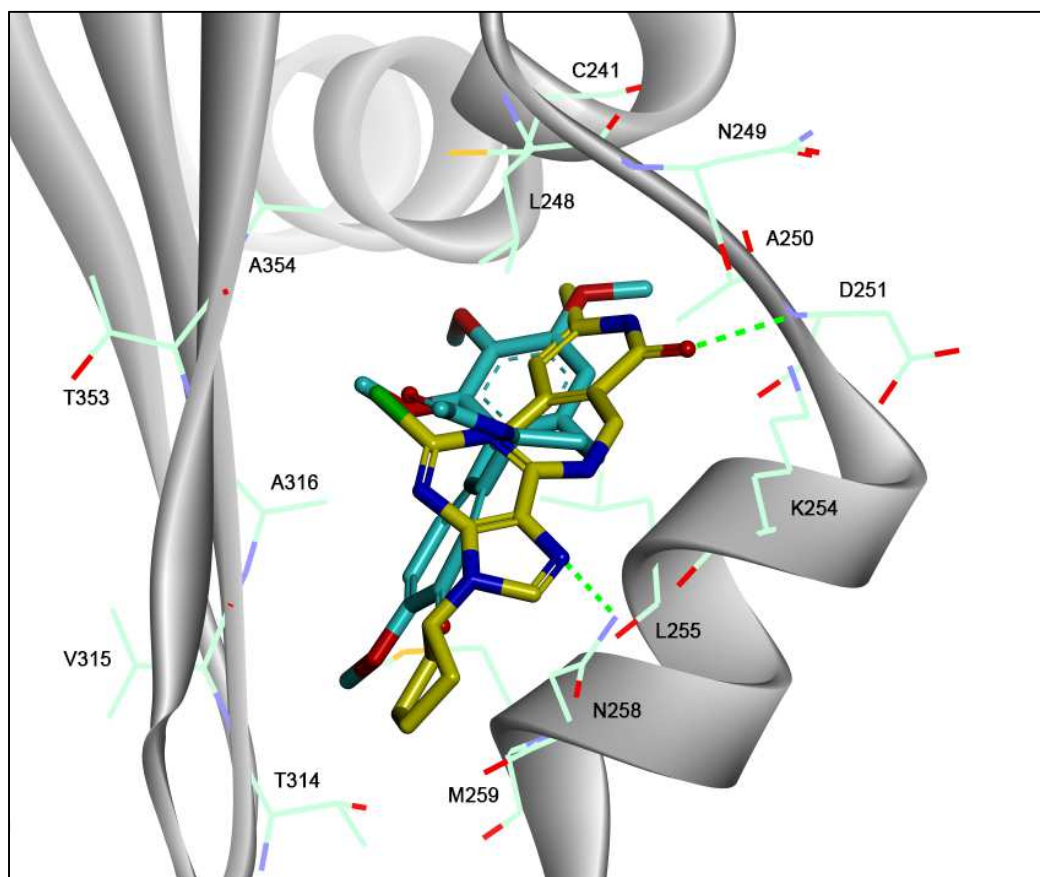


Fig. 4 Predicted binding mode of SKLB0533 (yellow stick) with tubulin (PDB code: 4O2B) and overlapping with Colchicine (blue stick). Hydrogen bonds are shown by green dashed lines.

2.5. Inhibition of other targets

Considering that the 2,6,9-trisubstituted purine fragment in SKLB0533 was often reported in kinase inhibitors, such as CDK1[34], CDK2[35], Src[36], AMPK[37] etc. Therefore, we tested the activity of SKLB0533 against a panel of 420 kinases by Eurofins Kinase Profiler. Here a single concentration (1 μ M) of SKLB0533 was used. The results showed that SKLB0533 had no activity against any of the kinases from the panel (**Fig. 5**, Supplementary **Tab. S1**). Furthermore, the

4,6-dimethylpyridin-2(1*H*)-one fragment in SKLB0533 was often reported in enhancer of zeste homologue 2 (EZH2) inhibitors[38, 39], we selected four structurally diverse compounds to test EZH2 inhibition activity. Compound **3b**, **4b2**, **5a** and SKLB0533 did not exhibit significant inhibition of EZH2 at 1 μ M or even at 10 μ M (Supplementary **Tab. S2**).

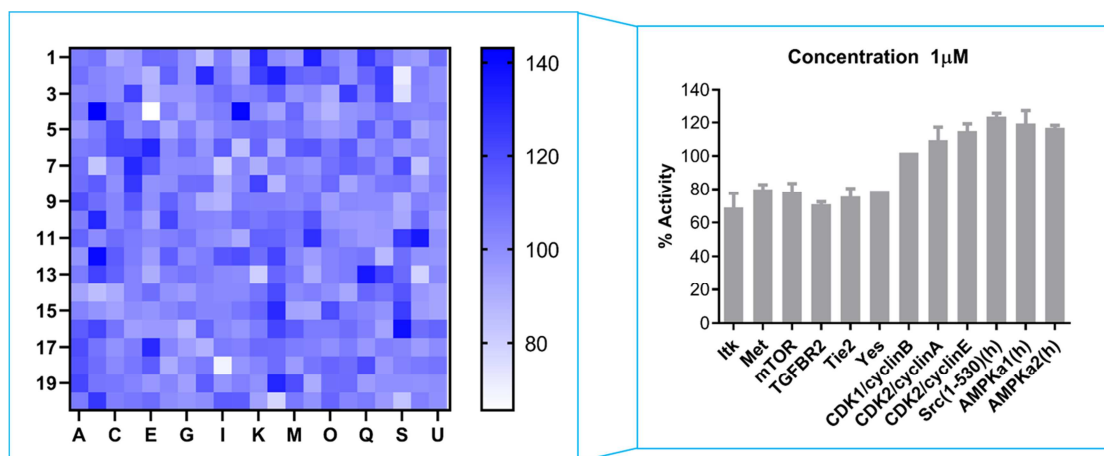


Fig. 5 Heat map of the inhibition rate against activity of 420 kinds of kinases.

These results indicate that SKLB0533 specifically inhibits of microtubule polymerization, and exhibits no activity against other potential targets, such as the 420 tested kinases and EZH2. These results suggest that SKLB0533 may have few toxic side effects since its off-target effects are minimal.

2.6. *In vitro* antiproliferative activities

We chose a panel of cancer cell lines of different histotypes to investigate the antiproliferative effect of SKLB0533. The results demonstrated that SKLB0533 obviously inhibited all the tested cell lines after 72 h of incubation, with an optimal inhibitory effect on the CRC cell lines at IC₅₀ values between 44.5 and 135.5 nM (**Tab. 3**). Thus, we decided to study the effect of SKLB0533 on CRC cells.

Tab. 3 Effects of SKLB0533 on cell viability.

Cell lines	Cell type	IC ₅₀ (nM)
HCT116	Colorectal carcinoma	57.5±4.60
SW620	Colorectal carcinoma	60.0±1.41
CT26	Colorectal carcinoma	45.5±2.48
SW480	Colorectal carcinoma	64.5±3.18
DLD-1	Colorectal carcinoma	135.5±6.72
HCT15	Colorectal carcinoma	61.0±8.49
HT29	Colorectal carcinoma	71.0±3.54
MDA-MB-231	Breast cancer	200.5±2.48
HepG2	Hepatocellular carcinoma	80.0±12.00
PLC/PRF/5	Hepatocellular carcinoma	286.0±9.19
A549	Lung cancer	98.0±8.00

Data are expressed as the mean±SEM for at least 2 independent experiments.

To evaluate the anticancer activity of SKLB0533 on CRC cells, the HCT116 and SW620 cell lines were exposed to graded concentrations of SKLB0533 for either 24 h, 48 h or 72 h, and caused a marked decrease in viability (**Fig. 6A and 6B**). These results demonstrate that SKLB0533 inhibits the proliferation of HCT116 and SW620 cells in a time and concentration dependent manner. Colony formation assays were performed to further validate the anti-proliferating effect of SKLB0533. Notably, colonies in treatment group were fewer and smaller than those in vehicle group (**Fig. 6C**), and when the concentration reached 50 nM, almost no colony formation was observed in SW620 cell lines.

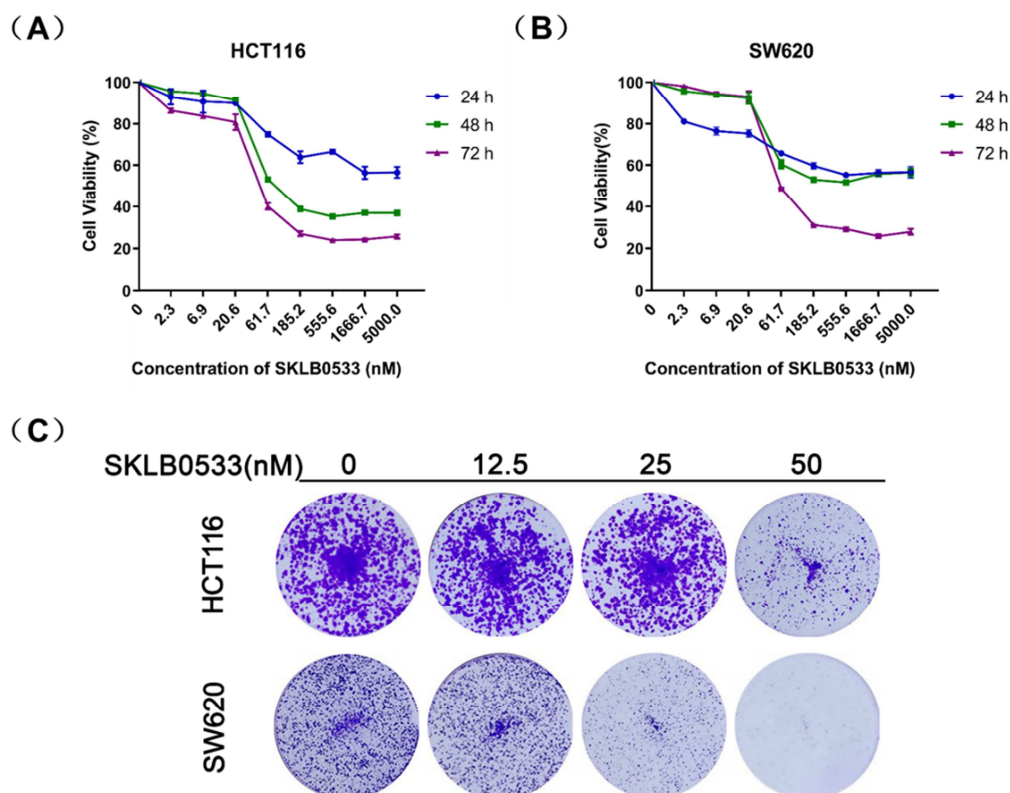


Fig. 6 SKLB0533 suppressed proliferation of HCT116 and SW620 cells. (A)(B) Tumour cells were treated with different concentrations of SKLB0533 for 24 h, 48 h or 72 h. MTT assays were performed to measure cell proliferation. (C) Effect of SKLB0533 on cell colony formation after two weeks of treatment.

2.7. Cell cycle arrest

Both microtubule stabilizers and destabilizers alter the tubulin-microtubule equilibrium causing mitotic arrest at the G2/M phase and ultimately apoptotic cell death. A flow cytometry analysis was performed to examine the effect of SKLB0533 on HCT116 and SW620 cell cycle progression (**Fig. 7A**). Treatment of SKLB0533 resulted in the gradual accumulation of cells in the G2/M phase of the cell cycle, and this accumulation occurred in a concentration-dependent manner, whereas the control

cells were mainly in the G1 phase. Thus, the cell cycle distribution indicated that SKLB0533 could arrest HCT116 and SW620 cells in the G2/M phase.

To gain insight into the molecular mechanism underlying cell cycle arrest, several cell cycle-related proteins were detected by western blot analysis. As shown in **Fig. 7B**, after treatment with SKLB0533 for 24 h, the expression of CyclinB1 and CDK1 were both upregulated. Furthermore, the level of cdc25c, which catalyses the dephosphorylation of pCDK1(Y15), was also upregulated. Then we observed a decrease in the level of pCDK1(Y15). These results suggest that high levels of CyclinB1-CDK1 complex induce the cell cycle to remain in the stage of G2/M transformation.

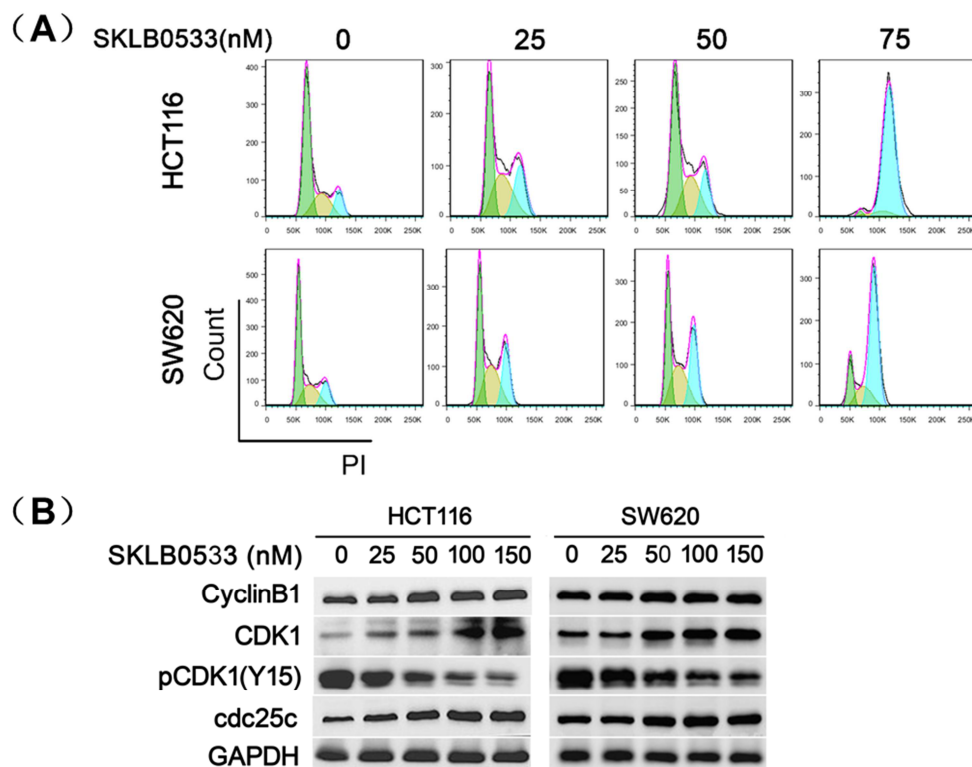


Fig. 7 SKLB0533 induced G2/M arrest in HCT116 and SW620 cells. (A) HCT116 and SW620 cell lines were treated with increasing doses of SKLB0533 (0, 25, 50 and

75 nM) for 24 h and were stained with 50 mg/mL propidium iodide (PI). (B) Effects of SKLB0533 on the expression of G2/M phase related regulator proteins. HCT116 and SW620 cell lines were treated with SKLB0533 for 24 h at the indicated concentrations (0, 25, 50, 100 and 150 nM).

2.8. Cell apoptosis analysis

Mitotic arrest of tumour cells by tubulin-directed agents is generally associated with cellular apoptosis. To investigate the effects of SKLB0533 inducing apoptosis, AnnexinV/PI staining was performed to further determine whether SKLB0533 had a pro-apoptotic effect on CRC cell lines. As shown in **Fig. 8A**, after exposure of HCT116 cells to SKLB0533 for 48 h, both early apoptotic cells (Q3) and late apoptotic cells (Q2) remarkably increased from 14.3% to 54.9% as the SKLB0533 concentration increased from 25 nM to 100 nM. Meanwhile, only a few apoptotic cells were detected in the control group. We also observed similar results in SW620 cells. These data suggested that SKLB0533 induces apoptosis of HCT116 and SW620 cells in a concentration-dependent manner.

Meanwhile, we also detected changes in several key proteins in the apoptosis pathway. As shown in **Fig. 8B**, caspase9, which is involved in the mitochondrial-mediated intrinsic apoptosis pathway, was activated after 48 h of SKLB0533 treatment, as we observed that the level of cleaved caspase9 increased in a dose-dependent manner. Additionally, the main executor of apoptosis, caspase3, was then cleaved and activated. The significant increase in the expression of cleaved

PARP further indicated that caspase3 was activated after 48 h of SKLB0533 treatment. We also detected the expression of some Bcl-2 family proteins, which were involved in regulating apoptosis. These results showed that the level of Bcl-2 decreased, while the level of Bax increased, in both cell lines.

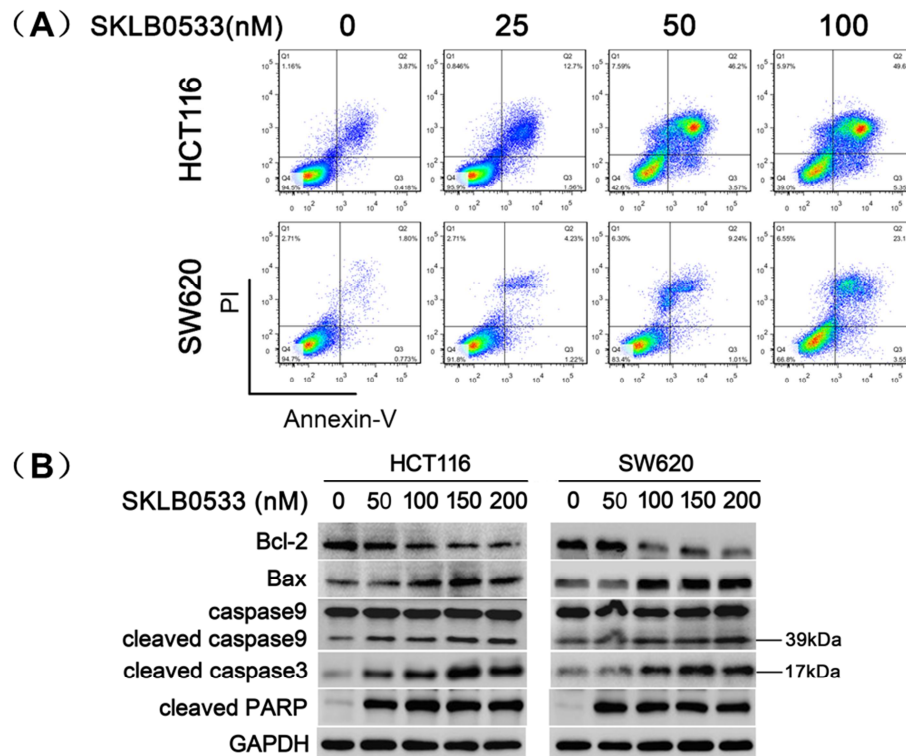


Fig. 8 SKLB0533 induced apoptosis of HCT116 and SW620 cells. (A) HCT116 and SW620 cells were treated with SKLB0533 for 48 h and apoptosis was detected by flow cytometry after Annexin V/PI staining. (B) Effects of SKLB0533 on the expression of apoptosis related regulator proteins. The levels of Bcl-2, Bax, cleaved caspase9, cleaved caspase3 and cleaved PARP were determined via western blot analysis.

2.9. *In vivo* antitumor efficacy in human xenografts of SKLB0533

To evaluate the *in vivo* therapeutic efficacy of SKLB0533, HCT116 colon cancer

cells were subcutaneously engrafted into nude mice to establish a xenograft model. Capecitabine, a first-line treatment for colorectal cancer, was selected as the positive reference. SKLB0533 was orally administered at 40 or 80 mg/kg once daily over a period of 4 weeks, at which point the tumour size reached approximately 100 mm³. As shown in **Fig. 9A, 9B and 9D**, oral administration of 40 and 80 mg/kg SKLB0533 once daily for 4 weeks showed TGI values of 39.9% and 71.6%, respectively, on day 28. However, under the same condition, the TGI from the group treated with 540 mg/kg capecitabine was only 61.6%. We also observed a significant reduction in tumour weight in **Fig. 9C**. These results indicate that the SKLB0533 potently and effectively inhibits colorectal tumour growth in xenograft models.

2.10. Preliminary safety profile of SKLB0533

To determine the potential toxicity of SKLB0533, we observed changes in body weight and determined the routine parameters and biochemical analysis of blood. As illustrated in **Fig. 10A and 10B**, no significant changes were observed in body weight, and the haematological and serum biochemical values were comparable with those of the vehicle group after 4 weeks SKLB0533 treatment. Moreover, microscopic examination of the heart, liver, spleen, lung and kidneys further showed that SKLB0533 (80 mg/kg) treatment did not cause obvious toxicity in mice (**Fig. 10C**).

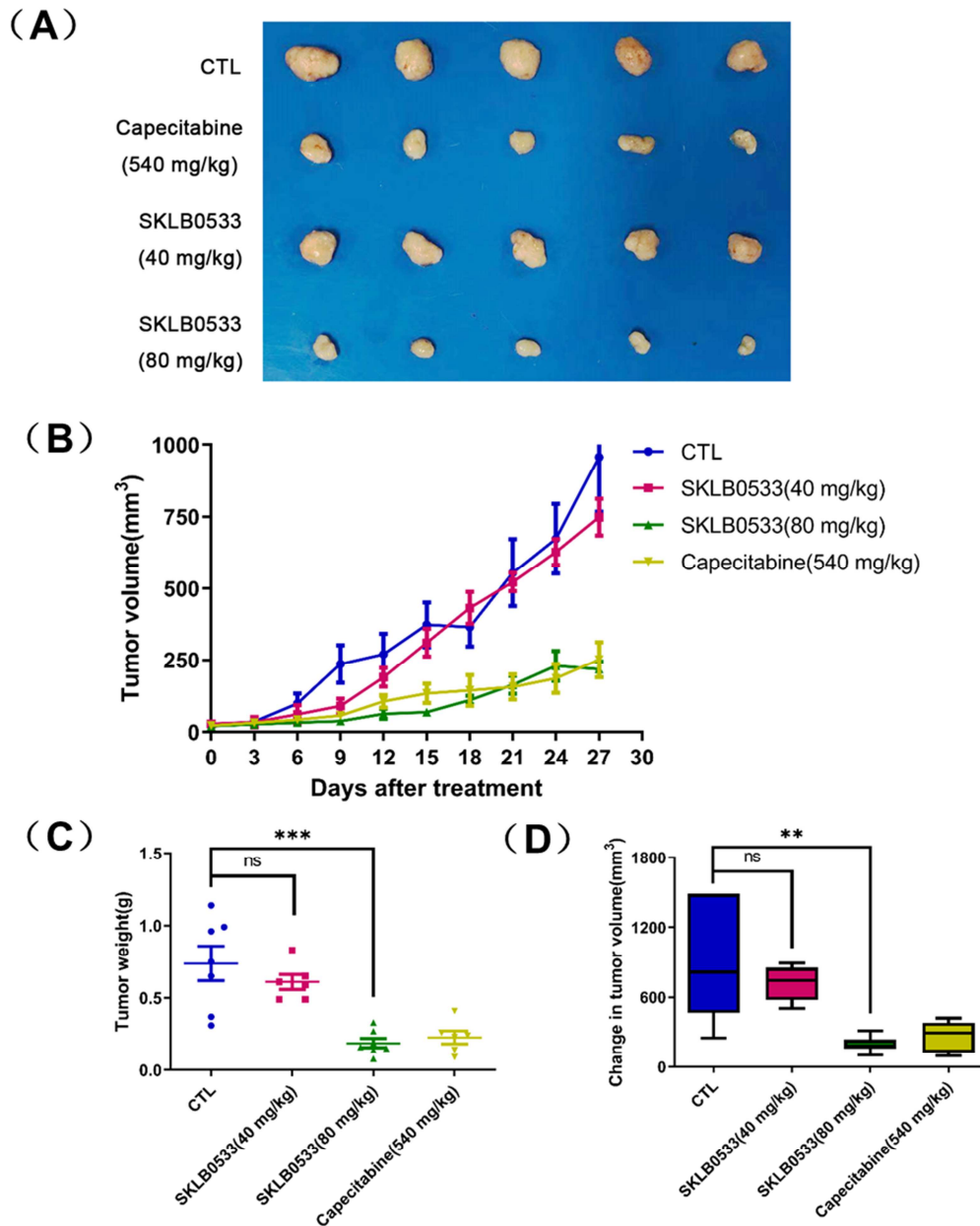


Fig. 9 Effects of SKLB0533 on the growth of HCT116 xenografts in BALB/c mice. BALB/c mice bearing HCT116 (n = 7) were orally treated with the vehicle control or SKLB0533 once every day for 4 weeks. (A) Images of excised tumours from each group. (B) Effects of SKLB0533 on tumour growth in a mouse xenograft. (C) Weight of tumours from sacrificed mice. (D) Change in tumour volume at day 28. Data are presented as the mean \pm SD of 7 mice. * $p < 0.05$, ** $p < 0.01$, *** $p < 0.001$.

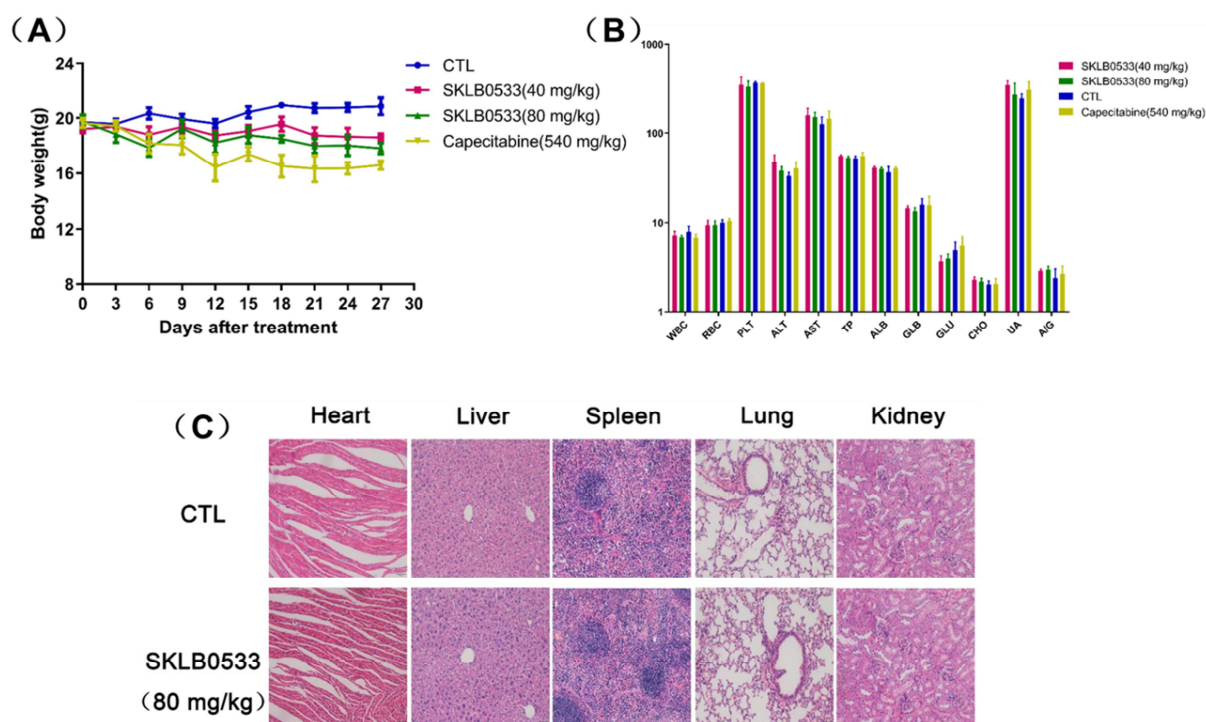


Fig. 10 Preliminary safety evaluation of SKLB0533 in BALB/c mice. (A) The differences in body weight between three treatment groups (SKLB0533 40 mg/kg, SKLB0533 80 mg/kg and Capecitabine) and the vehicle group were not significant. Data are expressed as the mean \pm SD (n=7). (B) SKLB0533 did not cause significant changes in routine blood analysis. The parameter units are as follows: WBC (white blood cell) and PLT (platelet), $10^9/L$; RBC (red blood cell), $10^{12}/L$; ALB (albumin), GLB (globulin) and TP (total protein), g/L; ALT (alanine transaminase) and AST (aspartate aminotransferase), U/L; UA (uric acid), μM ; CHO (cholesterol) and GLU (glucose), mM. A/G, ALB/ GLB. (C) Paraformaldehyde fixed organs (the heart, liver, spleen, lungs and kidneys) were processed for paraffin embedding and then stained with hematoxylin and eosin. The images shown are representatives from each group. Scale bars represent 50 μm .

3. Conclusion

In this study, we designed, synthesized and evaluated a series of novel 3-(((9*H*-purin-6-yl)amino)methyl)-4,6-dimethylpyridin-2(1*H*)-one derivatives as potential inhibitors of tubulin polymerization using bioelectronic isosteric strategy. SKLB0533 displayed the most potent activity against a wide variety of cancer cell lines, with an optimal inhibitory effect on CRC cell lines. The immunofluorescence analysis and tubulin polymerization assay results indicated that SKLB0533 could effectively inhibit tubulin polymerization. Furthermore, this compound exhibited no activity against 420 different kinases and EZH2, indicating considerable selectivity. In mechanism, SKLB0533 could disturb the dynamics of tubulin, arrest the cell cycle in the G2/M phase and induce apoptosis in HCT116 and SW620 cells. Moreover, SKLB0533 was demonstrated significant antitumor efficacy in the HCT116-xenograft mode without overt toxicities. In conclusion, these results highlighted the SKLB0533 as a promising anti-tubulin agent for the treatment of CRC.

4. Experimental section

4.1. Chemistry

Unless otherwise noted, all materials were obtained from commercial suppliers and used without further purification. Melting point (mp) was measured on hot-stage microscope (Shanghai Precision Scientific Instruments Co., Ltd, X-4). The ^1H and ^{13}C NMR spectra were recorded on a Bruker Avance 400 spectrometer at 25 °C using $\text{DMSO-}d_6$, CD_3OD or CDCl_3 as the solvent. Chemical shifts (δ) are reported in ppm

relative to Me₄Si (internal standard), coupling constants (*J*) are reported in hertz, and peak multiplicity are reported as s (singlet), d (doublet), t (triplet), q (quartet), m (multiplet), or br s (broad singlet). High resolution mass analysis was performed on a Waters Q-TOF Premier mass spectrometer with electron spray ionization (ESI). Thin layer chromatography (TLC) was performed on 0.20 mm silica gel F-254 plates (Qingdao Haiyang Chemical, China). Visualization of TLC was accomplished with UV light and/or aqueous potassium permanganate or I₂ in a silica gel. Column chromatography was performed using silica gel 60 of 300-400 mesh (Qingdao Haiyang Chemical, China).

4.1.1. The representative procedure for the preparation of 2,6-dichloro-9-substituted-9*H*-purine derivatives (**2a-2c**).

2,6-dichloro-9-isopropyl-9*H*-purine (**2a**). 2,6-dichloro-9*H*-purine (1.0 g, 5.29 mmol), and potassium carbonate (K₂CO₃) (2.193 g, 15.87 mmol) were dissolved in 20 ml anhydrous DMSO. Iodopropane (2.64 mL, 26.45 mmol) was added dropwise at 15 °C. The reaction mixture was stirred at 15 °C overnight. Upon completion of the reaction, the reaction solution was poured into ice water, and a white solid precipitated. The solution was filtered and dried under a vacuum to give 1.1 g of light yellow solid. Yield: 90.02%. ¹H NMR (400 MHz, DMSO-*d*₆) δ 8.86 (s, 1H), 4.83 (p, *J* = 6.8 Hz, 1H), 1.56 (d, *J* = 6.8 Hz, 6H).

2,6-dichloro-9-(pentan-3-yl)-9*H*-purine (**2b**). White solid, yield: 81.75%. ¹H

NMR (400 MHz, DMSO- d_6) δ 8.85 (s, 1H), 4.38 (tt, J = 8.8, 5.6 Hz, 1H), 2.10 -1.85 (m, 4H), 0.72 (t, J = 7.4 Hz, 6H).

2,6-dichloro-9-cyclopentyl-9H-purine (**2c**). White solid, yield: 58.82%. ^1H NMR (400 MHz, DMSO- d_6) δ 8.82 (s, 1H), 4.93 (p, J = 7.4 Hz, 1H), 2.20 (dq, J = 12.7, 6.7 Hz, 2H), 2.02 (dq, J = 13.6, 7.1 Hz, 2H), 1.89 (m, 2H), 1.77 – 1.64 (m, 2H).

4.1.2. The representative procedure for the preparation of 3-(((2-chloro-9-substituted-9H-purin-6-yl)amino)methyl)-4,6-dimethylpyridin-2(1H)-one derivatives (**3a-3c**).

3-(((2-chloro-9-isopropyl-9H-purin-6-yl)amino)methyl)-4,6-dimethylpyridin-2(1H)-one (**3a**). 2,6-dichloro-9-isopropyl-9H-purine (**2a**) (540 mg, 2.34 mmol), 3-(aminomethyl)-4,6-dimethylpyridin-2(1H)-one (427 mg, 2.81 mmol, obtained following the reference procedure [40]), and triethylamine (1.626 mL, 11.7 mmol) were added to ethanol (10 mL), and the reaction solution was reacted under reflux at 80 ° C for 6 h. A white solid precipitated during the reaction. After the reaction was completed, the suspension obtained was filtered and washed with cold ethanol (10 mL) to afford a solid product. The crude product was purified by silica gel column chromatography to afford target compounds as white solid with yield 50.52%, mp 141-143 °C. ^1H NMR (400 MHz, DMSO- d_6) δ 11.52 (s, 1H), 8.24 (s, 1H), 7.73 (t, J = 5.7 Hz, 1H), 5.87 (s, 1H), 4.66 (m, J = 6.7 Hz, 1H), 4.45 (d, J = 5.3 Hz, 2H), 2.28 (s, 3H), 2.11 (s, 3H), 1.49 (d, J = 6.8 Hz, 6H). ^{13}C NMR (101 MHz, Chloroform- d) δ

165.35, 155.06, 154.13, 150.85, 149.71, 143.23, 137.16, 121.96, 119.10, 109.66, 46.77, 37.00, 22.80 (2C), 19.70, 18.87. HRMS (ESI): calcd. for $C_{16}H_{19}ClN_6O$ $[M+Na]^+$: 369.1207, found: 369.1204.

3-(((2-chloro-9-(pentan-3-yl)-9*H*-purin-6-yl)amino)methyl)-4,6-dimethylpyridin-2(1*H*)-one (**3b**). White solid, yield: 64.23%, mp 224-225 °C. 1H NMR (400 MHz, DMSO- d_6) δ 11.52 (s, 1H), 8.21 (s, 1H), 7.75 (t, $J = 5.7$ Hz, 1H), 5.88 (s, 1H), 4.44 (d, $J = 5.2$ Hz, 2H), 4.19 (m, 1H), 2.29 (s, 3H), 2.11 (s, 3H), 1.90 (ddt, $J = 18.1, 14.1, 7.1$ Hz, 4H), 0.69 (t, $J = 7.3$ Hz, 6H). ^{13}C NMR (101 MHz, Chloroform- d) δ 165.34, 155.02, 154.15, 150.82, 143.17, 138.22, 122.06, 109.66, 58.83, 36.96, 27.78 (2C), 19.72, 18.89, 10.49 (2C). HRMS (ESI): calcd. for $C_{18}H_{23}ClN_6O$ $[M+Na]^+$: 397.1520, found: 397.1525.

3-(((2-chloro-9-cyclopentyl-9*H*-purin-6-yl)amino)methyl)-4,6-dimethylpyridin-2(1*H*)-one (**3c**). White solid, yield: 82.76%, mp 220-221 °C. 1H NMR (400 MHz, DMSO- d_6) δ 11.52 (s, 1H), 8.21 (s, 1H), 7.73 (t, $J = 7.9$ Hz, 1H), 5.87 (s, 1H), 4.82 – 4.71 (m, 1H), 4.45 (d, $J = 5.3$ Hz, 2H), 2.28 (s, 3H), 2.11 (m, 5H), 1.89 (m, 2H), 1.68 (m, 2H). ^{13}C NMR (101 MHz, Chloroform- d) δ 164.87, 154.88, 154.16, 151.31, 150.05, 143.01, 137.78, 121.93, 118.68, 109.82, 55.70, 36.75, 32.85 (2C), 23.75 (2C), 19.65, 18.64. HRMS (ESI): calcd. for $C_{18}H_{21}ClN_6O$ $[M+Na]^+$: 395.1363, found: 395.1362.

4.1.3. The representative procedure for the preparation of 3-(((2-substituted-9-

substituted -9*H*-purin-6-yl)amino)methyl)-4,6-dimethylpyridin-2(1*H*)-one derivatives (**4a1-4a7;4b1-4b7;4c1-4c7**).

3-(((9-isopropyl-2-(4-(trifluoromethoxy)phenyl)-9*H*-purin-6-yl)amino)methyl)-4,6 dimethylpyridin-2(1*H*)-one (**4a1**). To a stirred solution of **3a** (140 mg, 0.40 mmol) in a dioxane–water mixture (16 mL/4 mL), (4-(trifluoromethoxy)phenyl) boronic acid pinacol ester (172.8 mg, 0.60 mmol) was added, followed by the addition of Na₂CO₃ (169.6 mg, 1.60 mmol). The solution was purged with argon for 15 min and then PdCl₂(dppf) • CH₂Cl₂ (29.2 mg, 0.04 mmol) was added and the solution was again purged with argon for an additional 10 min. The reaction mixture was stirred at 100 °C for 5 h. After completion (monitored by TLC), the reaction mixture was diluted with water and extracted with 10% MeOH/DCM. The combined organic layers were dried over anhydrous sodium sulphate, filtered and concentrated under reduced pressure. The crude compound was purified by column chromatography eluting with MeOH/DCM to afford the desired compound **4a1** as a white solid. Yield: 53.40%, mp 264-266 °C. ¹H NMR (400 MHz, DMSO-*d*₆) δ 11.55 (s, 1H), 8.55 (d, *J* = 8.4 Hz, 2H), 8.25 (s, 1H), 7.47 (d, *J* = 8.4 Hz, 2H), 7.34 (t, *J* = 5.7 Hz, 1H), 5.85 (s, 1H), 4.83 (m, *J* = 6.8 Hz, 1H), 4.71 (d, *J* = 5.3 Hz, 2H), 2.26 (s, 3H), 2.11 (s, 3H), 1.58 (d, *J* = 6.7 Hz, 6H). ¹³C NMR (101 MHz, Chloroform-*d*) δ 165.29, 157.42, 154.43, 150.25, 142.95, 137.54, 129.67 (2C), 122.78, 120.35 (2C), 109.44, 46.90, 29.70, 22.76 (2C), 19.79, 18.91. HRMS (ESI): calcd. for C₂₃H₂₃F₃N₆O₂ [M+H]⁺: 473.1913, found: 473.1914.

3-(((9-isopropyl-2-(4-morpholinophenyl)-9*H*-purin-6-yl)amino)methyl)-4,6 dimethyl-

pyridin-2(1*H*)-one (**4a2**). Brown solid, yield: 68.06%, mp 190-192 °C. ¹H NMR (400 MHz, Chloroform-*d*) δ 11.87 (s, 1H), 8.44 (d, *J* = 8.5 Hz, 2H), 7.71 (s, 1H), 6.97 (d, *J* = 8.9 Hz, 2H), 6.67 (t, *J* = 5.7 Hz 1H), 5.86 (s, 1H), 4.96 (d, *J* = 5.3 Hz, 2H), 4.88 (m, *J* = 6.8 Hz, 1H), 3.89 (t, *J* = 5.9, 3.7 Hz, 4H), 3.30 – 3.20 (t, 4H), 2.41 (s, 3H), 2.30 (s, 3H), 1.61 (d, *J* = 6.8 Hz, 6H). ¹³C NMR (101 MHz, Chloroform-*d*) δ 164.80, 158.93, 154.05, 152.15, 150.97, 149.88, 142.73, 137.02, 130.65, 129.27 (2C), 122.83, 118.16, 114.65 (2C), 109.74, 66.77 (2C), 48.78 (2C), 46.75, 35.97, 22.59 (2C), 19.73, 18.49. HRMS (ESI): calcd. for C₂₆H₃₁N₇O₂ [M+H]⁺: 474.2617, found: 474.2617.

3-(((9-isopropyl-2-(3-morpholinophenyl)-9*H*-purin-6-yl)amino)methyl)-4,6-dimethylpyridin-2(1*H*)-one (**4a3**). Off-white solid, yield: 57.59%, mp 146-148 °C. ¹H NMR (400 MHz, DMSO-*d*₆) δ 11.55 (s, 1H), 8.22 (s, 1H), 8.06 (s, 1H), 7.91 (d, *J* = 7.7 Hz, 1H), 7.33 (t, *J* = 7.9 Hz, 1H), 7.15 (t, *J* = 5.7 Hz, 1H), 7.04 (d, *J* = 8.4 Hz, 1H), 5.86 (s, 1H), 4.83 (m, *J* = 6.8 Hz, 1H), 4.73 (d, *J* = 5.3 Hz, 2H), 3.79 (t, *J* = 4.7 Hz, 4H), 3.19 (t, *J* = 4.8 Hz, 4H), 2.30 (s, 3H), 2.11 (s, 3H), 1.57 (d, *J* = 6.7 Hz, 6H). ¹³C NMR (101 MHz, Chloroform-*d*) δ 165.31, 158.76, 154.36, 151.35, 142.88, 140.26, 137.32, 128.89, 123.01, 120.40, 117.15, 115.65, 109.33, 67.08 (2C), 49.73 (2C), 46.66, 22.84 (2C), 19.89, 18.95. HRMS (ESI): calcd. for C₂₆H₃₁N₇O₂ [M+H]⁺: 474.2617, found: 474.2613.

3-(((9-isopropyl-2-(4-(morpholinomethyl)phenyl)-9*H*-purin-6-yl)amino)methyl)-4,6-dimethylpyridin-2(1*H*)-one (**4a4**). Light yellow solid, yield: 21.68%, mp

240-242 °C. ^1H NMR (400 MHz, DMSO- d_6) δ 11.55 (s, 1H), 8.39 (d, J = 7.8 Hz, 2H), 8.22 (s, 1H), 7.41 (d, J = 8.0 Hz, 2H), 7.19 (t, J = 5.7 Hz, 1H), 5.85 (s, 1H), 4.87 – 4.77 (m, 1H), 4.71 (d, J = 5.3 Hz, 2H), 3.59 (t, J = 4.6 Hz, 4H), 3.52 (s, 2H), 2.38 (t, J = 4.5 Hz, 4H), 2.27 (s, 3H), 2.11 (s, 3H), 1.57 (d, J = 6.7 Hz, 6H). ^{13}C NMR (101 MHz, Chloroform- d) δ 165.53, 158.57, 154.40, 150.30, 143.18, 139.02, 138.42, 137.29, 129.04 (2C), 128.11 (2C), 122.79, 119.20, 109.50, 67.05 (2C), 63.34, 53.68 (2C), 46.76, 29.70, 22.78 (2C), 19.85, 18.87. HRMS (ESI): calcd. for $\text{C}_{27}\text{H}_{33}\text{N}_7\text{O}_2$ $[\text{M}+\text{H}]^+$: 488.2774, found: 488.2770.

3-(((9-isopropyl-2-(4-(4-methylpiperazin-1-yl)phenyl)-9H-purin-6-yl)amino)methyl)-4,6-dimethylpyridin-2(1H)-one (**4a5**). Brown solid, yield: 59.69%, mp 202-204 °C. ^1H NMR (400 MHz, Chloroform- d) δ 12.20 (s, 1H), 8.42 (d, J = 8.6 Hz, 2H), 7.70 (s, 1H), 6.99 (d, J = 8.0 Hz, 2H), 6.71 (t, J = 5.7 Hz 1H), 5.87 (s, 1H), 4.95 (d, J = 5.3 Hz, 2H), 4.88 (m, J = 6.7 Hz, 1H), 3.32 (t, J = 5.0 Hz, 4H), 2.60 (t, J = 5.0 Hz, 4H), 2.41 (s, 3H), 2.36 (s, 3H), 2.31 (s, 3H), 1.60 (d, J = 6.8 Hz, 6H). ^{13}C NMR (101 MHz, Chloroform- d) δ 165.49, 158.76, 154.32, 152.13, 150.25, 143.03, 136.86, 130.49, 129.22 (2C), 122.98, 118.78, 114.94 (2C), 109.45, 77.24, 55.05 (2C), 48.60 (2C), 46.62, 46.19, 22.77 (2C), 19.88, 18.89. HRMS (ESI): calcd. for $\text{C}_{27}\text{H}_{34}\text{N}_8\text{O}$ $[\text{M}+\text{H}]^+$: 487.2934, found: 487.2929.

3-(((9-isopropyl-2-(6-(4-methylpiperazin-1-yl)pyridin-3-yl)-9H-purin-6-yl)amino)methyl)-4,6-dimethylpyridin-2(1H)-one (**4a6**). Brown solid, yield: 56.85%, mp

206-207 °C. ^1H NMR (400 MHz, Chloroform-*d*) δ 11.88 (s, 1H), 9.32 (d, J = 2.3 Hz, 1H), 8.54 (dd, J = 8.9, 2.4 Hz, 1H), 7.69 (t, J = 5.7 Hz, 1H), 6.81 – 6.60 (m, 2H), 5.87 (s, 1H), 4.93 (d, J = 5.3 Hz, 2H), 4.83 (m, J = 6.8 Hz, 1H), 3.67 (t, J = 5.1 Hz, 4H), 2.55 (t, J = 5.1 Hz, 4H), 2.40 (s, 3H), 2.36 (s, 3H), 2.30 (s, 3H), 1.61 (d, J = 6.8 Hz, 6H). ^{13}C NMR (101 MHz, Chloroform-*d*) δ 164.68, 159.61, 157.60, 154.09, 150.92, 148.60, 142.63, 137.44, 137.13, 124.63, 122.90, 118.33, 109.84, 106.19, 54.65 (2C), 46.95, 45.91, 44.92 (2C), 22.55 (2C), 19.79, 18.54, 18.01. HRMS (ESI): calcd. for $\text{C}_{26}\text{H}_{33}\text{N}_9\text{O}$ $[\text{M}+\text{H}]^+$: 488.2886, found: 488.2878.

Tert-butyl

4-(5-(6-(((4,6-dimethyl-2-oxo-1,2-dihydropyridin-3-yl)methyl)amino)-9-isopropyl-9H-purin-2-yl)pyridin-2-yl)piperazine-1-carboxylate (**4a7**). Off-white solid, yield: 60.42%, mp 186-188 °C. ^1H NMR (400 MHz, DMSO-*d*₆) δ 11.56 (s, 1H), 9.16 (s, 1H), 8.49 (d, J = 7.8 Hz, 1H), 8.17 (s, 1H), 7.15 (t, J = 5.7 Hz, 1H), 6.91 (d, J = 9.0 Hz, 1H), 5.85 (s, 1H), 4.79 (m, J = 6.7 Hz, 1H), 4.69 (d, J = 5.3 Hz, 2H), 3.60 (t, J = 4.6 Hz, 4H), 3.45 (t, J = 5.2 Hz, 4H), 2.28 (s, 3H), 2.10 (s, 3H), 1.56 (d, J = 6.8 Hz, 6H), 1.44 (s, 9H). ^{13}C NMR (101 MHz, Chloroform-*d*) δ 165.55, 159.50, 157.40, 154.85, 154.35, 150.25, 148.83, 143.21, 137.34, 137.01, 125.05, 122.73, 118.96, 109.47, 105.95, 79.98, 77.26, 46.88 (2C), 45.07 (2C), 28.45 (3C), 22.66 (2C), 19.88, 18.85. HRMS (ESI): calcd. for $\text{C}_{30}\text{H}_{39}\text{N}_9\text{O}_3$ $[\text{M}+\text{H}]^+$: 574.3254, found: 574.3252.

4,6-dimethyl-3-(((9-(pentan-3-yl)-2-(4-(trifluoromethoxy)phenyl)-9H-purin-6-yl)

amino)methyl)pyridin-2(1*H*)-one (**4b1**). White solid, yield: 56.87%, mp 204-206 °C. ¹H NMR (400 MHz, DMSO-*d*₆) δ 11.56 (s, 1H), 8.53 (d, *J* = 8.3 Hz, 2H), 8.21 (s, 1H), 7.47 (d, *J* = 8.4 Hz, 2H), 7.34 (t, *J* = 7.9 Hz, 1H), 5.86 (s, 1H), 4.70 (d, *J* = 5.3 Hz, 2H), 4.34 (m, *J* = 9.8, 4.7 Hz, 1H), 2.28 (s, 3H), 2.11 (s, 3H), 2.07 – 1.87 (m, 4H), 0.73 (t, *J* = 7.3 Hz, 6H). ¹³C NMR (101 MHz, Chloroform-*d*) δ 165.27, 157.46, 154.30, 150.58, 150.22, 143.13, 138.86, 137.95, 129.69 (2C), 122.66, 121.81, 120.32 (2C), 118.96, 109.65, 77.26, 59.50, 27.70 (2C), 19.77, 18.72, 10.71 (2C). HRMS (ESI): calcd. for C₂₅H₂₇F₃N₆O₂ [M+Na]⁺: 523.2046, found: 523.2044.

4,6-dimethyl-3-(((2-(4-morpholinophenyl)-9-(pentan-3-yl)-9*H*-purin-6-yl)amino)methyl)pyridin-2(1*H*)-one (**4b2**). Brown solid, yield: 64.23%, mp 242-243 °C. ¹H NMR (400 MHz, DMSO-*d*₆) δ 11.56 (s, 1H), 8.29 (d, *J* = 8.5 Hz, 2H), 8.11 (s, 1H), 7.07 (t, *J* = 7.9 Hz, 1H), 7.01 (d, *J* = 8.8 Hz, 2H), 5.86 (s, 1H), 4.70 (d, *J* = 5.3 Hz, 2H), 4.32 (m, *J* = 5.2 Hz, 1H), 3.76 (t, *J* = 4.8 Hz, 4H), 3.21 (t, *J* = 4.9 Hz, 4H), 2.30 (s, 3H), 2.11 (s, 3H), 2.09 – 1.86 (m, 4H), 0.72 (t, *J* = 7.3 Hz, 6H). ¹³C NMR (101 MHz, Chloroform-*d*) δ 165.59, 158.59, 154.27, 152.15, 150.28, 143.15, 138.28, 131.04, 129.28 (2C), 122.94, 118.72, 114.67 (2C), 109.52, 66.87 (2C), 59.23, 48.93 (2C), 27.68 (2C), 24.89, 19.88, 18.86, 10.77 (2C). HRMS (ESI): calcd. for C₂₈H₃₅N₇O₂ [M+Na]⁺: 524.2750, found: 524.2753.

4,6-dimethyl-3-(((2-(3-morpholinophenyl)-9-(pentan-3-yl)-9*H*-purin-6-yl)amino)methyl)pyridin-2(1*H*)-one (**4b3**). Light yellow solid, yield: 29.87%, mp

170-172 °C. ^1H NMR (400 MHz, DMSO- d_6) δ 11.5(s, 1H), 8.17 (s, 1H), 8.04 (s, 1H), 7.89 (d, J = 7.7 Hz, 1H), 7.33 (t, J = 7.9 Hz, 1H), 7.20 (s, 1H), 7.04 (d, J = 8.0, 2.6 Hz, 1H), 5.85 (s, 1H), 4.73 (d, J = 5.3 Hz, 2H), 4.33 (m, J = 9.6, 4.8 Hz, 1H), 3.79 (t, J = 5.9, 3.6 Hz, 4H), 3.18 (t, J = 4.9 Hz, 4H), 2.31 (s, 3H), 2.11 (s, 3H), 2.09 – 1.88 (m, 4H), 0.72 (t, J = 7.3 Hz, 6H). ^{13}C NMR (101 MHz, Chloroform- d) δ 164.72, 158.96, 154.01, 151.23, 150.61, 142.60, 140.08, 138.67, 128.87, 122.97, 120.57, 118.50, 117.37, 115.78, 109.70, 77.29, 66.97 (2C), 59.26, 49.74 (2C), 27.69 (2C), 19.80, 18.54, 10.61 (2C). HRMS (ESI): calcd. for $\text{C}_{28}\text{H}_{35}\text{N}_7\text{O}_2$ $[\text{M}+\text{Na}]^+$: 524.2750, found: 524.2753.

4,6-dimethyl-3-(((2-(4-(morpholinomethyl)phenyl)-9-(pentan-3-yl)-9H-purin-6-yl)amino)methyl)pyridin-2(1H)-one (**4b4**). Off-white solid, yield: 58.10%, mp 224-225 °C. ^1H NMR (400 MHz, DMSO- d_6) δ 11.56 (s, 1H), 8.37 (d, J = 7.9 Hz, 2H), 8.17 (s, 1H), 7.40 (d, J = 8.1 Hz, 2H), 7.20 (t, J = 7.9 Hz, 1H), 5.86 (s, 1H), 4.71 (d, J = 5.3 Hz, 2H), 4.34 (m, 1H), 3.59 (t, J = 4.6 Hz, 4H), 3.52 (s, 2H), 2.38 (t, J = 4.9 Hz, 4H), 2.29 (s, 3H), 2.11 (s, 3H), 2.07 – 1.86 (m, 4H), 0.72 (t, J = 7.3 Hz, 6H). ^{13}C NMR (101 MHz, Chloroform- d) δ 164.74, 158.63, 150.70, 142.53, 138.66, 138.59, 138.38, 130.69, 129.14 (2C), 128.15 (2C), 122.97, 115.10, 109.65, 66.88 (2C), 63.27, 59.37, 53.54 (2C), 27.68 (2C), 19.78, 18.63, 10.66 (2C). HRMS (ESI): calcd. for $\text{C}_{29}\text{H}_{37}\text{N}_7\text{O}_2$ $[\text{M}+\text{Na}]^+$: 538.2907, found: 538.2906.

4,6-dimethyl-3-(((2-(4-(4-methylpiperazin-1-yl)phenyl)-9-(pentan-3-yl)-9H-purin-6-y

l)amino)methyl)pyridin-2(1*H*)-one (**4b5**). White solid, yield: 53.86%, mp 179-180. ¹H NMR (400 MHz, DMSO-*d*₆) δ 11.56 (s, 1H), 8.27 (d, *J* = 8.4 Hz, 2H), 8.10 (s, 1H), 7.06 (t, *J* = 5.7 Hz, 1H), 7.00 (d, *J* = 8.7 Hz, 2H), 5.86 (s, 1H), 4.70 (d, *J* = 5.3 Hz, 2H), 4.31 (m, *J* = 5.1 Hz, 1H), 3.24 (t, *J* = 5.0 Hz, 4H), 2.46 (t, *J* = 5.1 Hz, 4H), 2.30 (s, 3H), 2.23 (s, 3H), 2.11 (s, 3H), 2.08 – 1.87 (m, 4H), 0.72 (t, *J* = 7.3 Hz, 6H). ¹³C NMR (101 MHz, DMSO-*d*₆) δ 163.95, 157.99, 154.26, 152.34, 143.18, 140.45, 129.17 (2C), 122.90, 114.62 (2C), 108.02, 59.12, 54.99 (2C), 47.93 (2C), 46.27, 27.39 (2C), 19.55, 18.65, 11.10 (2C). HRMS (ESI): calcd. for C₂₉H₃₈N₈O [M+Na]⁺: 537.3067, found: 537.3073.

4,6-dimethyl-3-(((2-(6-(4-methylpiperazin-1-yl)pyridin-3-yl)-9-(pentan-3-yl)-9*H*-purin-6-yl)amino)methyl)pyridin-2(1*H*)-one (**4b6**). Brown solid, yield: 61.00%, mp 147-148 °C. ¹H NMR (400 MHz, DMSO-*d*₆) δ 11.56 (s, 1H), 9.13 (s, 1H), 8.43 (d, *J* = 8.9 Hz, 1H), 8.11 (s, 1H), 7.14 (t, *J* = 5.7 Hz, 1H), 6.90 (d, *J* = 9.0 Hz, 1H), 5.86 (s, 1H), 4.69 (d, *J* = 5.3 Hz, 2H), 4.31 (m, *J* = 4.8 Hz, 1H), 3.59 (t, *J* = 5.1 Hz, 4H), 2.41 (t, *J* = 5.0 Hz, 4H), 2.29 (s, 3H), 2.23 (s, 3H), 2.11 (s, 3H), 2.09 – 1.86 (m, 4H), 0.72 (t, *J* = 7.3 Hz, 6H). ¹³C NMR (101 MHz, Chloroform-*d*) δ 165.27, 159.67, 157.48, 154.20, 150.52, 148.76, 143.03, 138.36, 137.32, 124.75, 122.81, 118.58, 109.63, 105.96, 59.49, 54.79 (2C), 46.11, 45.09 (2C), 27.60 (2C), 19.88, 18.74, 10.74 (2C). HRMS (ESI): calcd. for C₂₈H₃₇N₉O [M+H]⁺: 516.3199, found: 516.3195.

tert-butyl

4-(5-(6-(((4,6-dimethyl-2-oxo-1,2-dihydropyridin-3-yl)methyl)amino)-9-(pentan-3-yl)-9H-purin-2-yl)pyridin-2-yl)piperazine-1-carboxylate (**4b7**). Off-white solid, yield: 58.76%, mp 150-152 °C. ¹H NMR (400 MHz, DMSO-*d*₆) δ 11.56 (s, 1H), 9.14 (s, 1H), 8.66 – 8.31 (d, *J* = 8.9 Hz, 1H), 8.12 (s, 1H), 7.16 (t, *J* = 5.7 Hz, 1H), 6.91 (d, *J* = 9.0 Hz, 1H), 5.86 (s, 1H), 4.69 (d, *J* = 5.3 Hz, 2H), 4.30 (m, *J* = 4.7 Hz, 1H), 3.60 (t, *J* = 6.8, 3.8 Hz, 4H), 3.45 (t, *J* = 6.8, 3.8 Hz, 4H), 2.29 (s, 3H), 2.11 (s, 3H), 2.08 – 1.89 (m, 4H), 1.43 (s, 9H), 0.72 (t, *J* = 7.3 Hz, 6H). ¹³C NMR (101 MHz, Chloroform-*d*) δ 165.50, 159.49, 157.32, 154.86, 154.29, 150.22, 148.83, 143.13, 138.41, 137.37, 125.13, 122.82, 118.87, 109.48, 105.96, 80.00, 59.53 (2C), 58.34, 45.10 (2C), 28.45 (3C), 27.63 (2C), 19.90, 18.87, 10.79 (2C). HRMS (ESI): calcd. for C₃₂H₄₃N₉O₃ [M+Na]⁺: 624.3387, found: 624.3386.

3-(((9-cyclopentyl-2-(4-(trifluoromethoxy)phenyl)-9H-purin-6-yl)amino)methyl)-4,6-dimethylpyridin-2(1H)-one (**4c1**). White solid, yield: 57.00%, mp 201-203 °C. ¹H NMR (400 MHz, DMSO-*d*₆) δ 11.55 (s, 1H), 8.54 (d, *J* = 8.4 Hz, 2H), 8.22 (s, 1H), 7.59 – 7.42 (d, *J* = 8.4 Hz, 2H), 7.34 (t, *J* = 7.9 Hz, 1H), 5.85 (s, 1H), 4.93 (p, *J* = 7.6 Hz, 1H), 4.71 (d, *J* = 5.3 Hz, 2H), 2.26 (s, 3H), 2.24 – 2.16 (m, 1H), 2.11 (s, 3H), 2.08 – 2.00 (m, 1H), 1.98 – 1.88 (m, 2H), 1.73 (m, 2H). ¹³C NMR (101 MHz, Chloroform-*d*) δ 165.54, 157.38, 154.41, 150.39, 150.29 – 150.16 (m), 143.37, 138.28, 138.00, 129.68 (2C), 122.53, 121.83, 120.34 (2C), 119.27, 109.56, 55.96, 32.75 (2C), 24.13 (2C), 19.75, 18.81. HRMS (ESI): calcd. for C₂₅H₂₅F₃N₆O₂ [M+Na]⁺: 521.1889, found: 521.1891.

3-(((9-cyclopentyl-2-(4-morpholinophenyl)-9*H*-purin-6-yl)amino)methyl)-4,6-dimethylpyridin-2(1*H*)-one (**4c2**). Brown solid, yield: 77.12%, mp 284-285 °C. ¹H NMR (400 MHz, DMSO-*d*₆) δ 11.54 (s, 1H), 8.31 (d, *J* = 8.4 Hz, 2H), 8.13 (s, 1H), 7.07 (t, *J* = 7.9 Hz, 1H), 7.02 (d, *J* = 8.6 Hz, 2H), 5.85 (s, 1H), 4.90 (t, *J* = 7.6 Hz, 1H), 4.70 (d, *J* = 5.3 Hz, 2H), 3.76 (t, *J* = 4.8 Hz, 4H), 3.21 (t, *J* = 4.9 Hz, 4H), 2.28 (s, 3H), 2.19 (m, 2H), 2.10 (s, 3H), 2.04 (m, 2H), 1.93 (m, 2H), 1.73 (m, 2H). ¹³C NMR (101 MHz, Chloroform-*d*) δ 164.83, 158.87, 154.10, 152.15, 150.80, 142.65, 137.71, 130.76, 129.29 (2C), 122.95, 118.31, 114.68 (2C), 109.64, 77.29, 66.81 (2C), 55.79, 48.83 (2C), 32.75 (2C), 24.09 (2C), 19.78, 18.60. HRMS (ESI): calcd. for C₂₈H₃₃N₇O₂ [M+H]⁺: 500.2774 found: 500.2769.

3-(((9-cyclopentyl-2-(3-morpholinophenyl)-9*H*-purin-6-yl)amino)methyl)-4,6-dimethylpyridin-2(1*H*)-one (**4c3**). Brown solid, yield: 72.56%, mp 153-155 °C. ¹H NMR (400 MHz, DMSO-*d*₆) δ 11.55 (s, 1H), 8.19 (s, 1H), 8.06 (s, 1H), 7.91 (d, *J* = 7.6 Hz, 1H), 7.33 (t, *J* = 7.9 Hz, 1H), 7.15 (s, 1H), 7.09 – 7.01 (m, 1H), 5.86 (s, 1H), 4.93 (m, 1H), 4.73 (d, *J* = 5.3 Hz, 2H), 3.79 (t, *J* = 4.8 Hz, 4H), 3.19 (t, *J* = 4.8 Hz, 4H), 2.30 (s, 3H), 2.24 – 2.15 (m, 2H), 2.11 (s, 3H), 2.08 – 2.00 (m, 2H), 1.95 (m, 2H), 1.74 (m, *J* = 7.8 Hz, 2H). ¹³C NMR (101 MHz, Chloroform-*d*) δ 164.73, 158.99, 154.07, 151.25, 150.69, 142.65, 140.04, 138.20, 128.91, 122.91, 120.52, 118.67, 117.38, 115.72, 109.70, 77.31, 66.97 (2C), 55.87, 49.71 (2C), 32.82 (2C), 24.19 (2C), 19.80, 18.56. HRMS (ESI): calcd. for C₂₈H₃₃N₇O₂ [M+Na]⁺: 522.2594, found: 522.2595.

3-(((9-cyclopentyl-2-(4-(morpholinomethyl)phenyl)-9*H*-purin-6-yl)amino)methyl)-4,6-dimethylpyridin-2(1*H*)-one (**4c4**). Off-white solid, yield: 40.16 %, mp 229-231 °C. ¹H NMR (400 MHz, DMSO-*d*₆) δ 11.55 (s, 1H), 8.38 (d, *J* = 7.8 Hz, 2H), 8.19 (s, 1H), 7.41 (d, *J* = 8.1 Hz, 2H), 7.20 (t, *J* = 7.9 Hz, 1H), 5.85 (s, 1H), 4.97 – 4.85 (m, 1H), 4.71 (d, *J* = 5.3 Hz, 2H), 3.59 (t, *J* = 4.6 Hz, 4H), 3.52 (s, 2H), 2.38 (t, *J* = 4.6 Hz, 4H), 2.27 (s, 3H), 2.24 – 2.15 (m, 2H), 2.11 (s, 3H), 2.08 – 2.00 (m, 2H), 1.97 – 1.87 (m, 2H), 1.73 (m, 2H). ¹³C NMR (101 MHz, Chloroform-*d*) δ 165.53, 158.56, 154.39, 150.29, 143.21, 139.00, 138.44, 138.05, 129.05 (2C), 128.12 (2C), 122.75, 119.18, 115.31, 109.50, 77.26, 67.05 (2C), 63.33, 55.84, 53.67 (2C), 32.81 (2C), 24.17 (2C), 19.84, 18.86. HRMS (ESI): calcd. for C₂₉H₃₅N₇O₂ [M+Na]⁺: 536.2750, found: 536.2743.

3-(((9-cyclopentyl-2-(4-(4-methylpiperazin-1-yl)phenyl)-9*H*-purin-6-yl)amino)methyl)-4,6-dimethylpyridin-2(1*H*)-one (**4c5**). White solid, yield: 65.26%, mp 171-173 °C. ¹H NMR (400 MHz, DMSO-*d*₆) δ 11.55 (s, 1H), 8.29 (d, *J* = 8.5 Hz, 2H), 8.12 (s, 1H), 7.05 (t, *J* = 7.9 Hz, 1H), 7.00 (d, *J* = 9.1 Hz, 1H), 5.85 (s, 1H), 4.90 (p, *J* = 7.5 Hz, 1H), 4.70 (d, *J* = 5.3 Hz, 2H), 3.24 (t, *J* = 5.0 Hz, 4H), 2.46 (t, *J* = 5.1 Hz, 4H), 2.28 (s, 3H), 2.23 (s, 3H), 2.21 – 2.14 (m, 2H), 2.10 (s, 3H), 2.00-2.06 (m, 2H), 1.97 – 1.89 (m, 2H), 1.73 (m, 2H). ¹³C NMR (101 MHz, Chloroform-*d*) δ 165.56, 158.74, 154.32, 152.12, 150.25, 143.14, 137.64, 130.52, 129.23 (2C), 122.91, 118.79, 114.95 (2C), 109.46, 77.26, 55.73, 55.04 (2C), 48.60 (2C), 46.19, 32.79 (2C), 24.18

(2C), 19.87, 18.86. HRMS (ESI): calcd. for $C_{29}H_{36}N_8O$ $[M+H]^+$: 513.3090 found: 513.3089.

3-(((9-cyclopentyl-2-(6-(4-methylpiperazin-1-yl)pyridin-3-yl)-9H-purin-6-yl)amino)methyl)-4,6-dimethylpyridin-2(1H)-one (**4c6**). Brown solid, yield: 62.17%, mp 224-226 °C. 1H NMR (400 MHz, DMSO- d_6) δ 11.55 (s, 1H), 9.14 (s, 1H), 8.45 (d, J = 8.9 Hz, 1H), 8.13 (s, 1H), 7.13 (t, J = 7.9 Hz, 1H), 6.90 (d, J = 9.0 Hz, 1H), 5.85 (s, 1H), 4.89 (m, 1H), 4.69 (d, J = 5.3 Hz, 2H), 3.59 (t, J = 5.0 Hz, 4H), 2.41 (t, J = 5.0 Hz, 4H), 2.27 (s, 3H), 2.23 (s, 3H), 2.21 – 2.14 (m, 2H), 2.10 (s, 3H), 2.07 – 2.01 (m, 2H), 1.97 – 1.89 (m, 2H), 1.72 (m, 2H). ^{13}C NMR (101 MHz, Chloroform- d) δ 165.45, 159.74, 157.48, 154.34, 150.22, 148.84, 143.05, 137.81, 137.23, 124.74, 122.85, 109.43, 105.87, 77.24, 56.02, 54.90 (2C), 46.25, 45.20 (2C), 32.64 (2C), 24.18 (2C), 19.91, 18.90. HRMS (ESI): calcd. for $C_{28}H_{35}N_9O$ $[M+Na]^+$: 536.2863, found: 536.2866.

tert-butyl 4-(5-(9-cyclopentyl-6-(((4,6-dimethyl-2-oxo-1,2-dihydropyridin-3-yl)methyl)amino)-9H-purin-2-yl)pyridin-2-yl)piperazine-1-carboxylate (**4c7**). Off-white solid, yield: 63.76%, mp 150-152 °C. 1H NMR (400 MHz, DMSO- d_6) δ 11.56 (s, 1H), 9.16 (s, 1H), 8.47 (d, J = 8.9 Hz, 1H), 8.13 (s, 1H), 7.15 (t, J = 7.9 Hz, 1H), 6.91 (d, J = 9.0 Hz, 1H), 5.85 (s, 1H), 4.89 (m, 1H), 4.69 (d, J = 5.3 Hz, 2H), 3.60 (dd, J = 7.0, 3.8 Hz, 4H), 3.45 (dd, J = 6.7, 3.9 Hz, 4H), 2.28 (s, 3H), 2.17 (m, 2H), 2.10 (s, 3H), 2.07 – 2.01 (m, 2H), 1.93 (m, 2H), 1.72 (m, 2H), 1.44 (s, 9H). ^{13}C NMR (101 MHz,

DMSO- d_6) δ 163.92, 159.53, 156.70, 154.44, 148.38, 143.18, 140.01, 137.25, 124.23, 122.84, 108.01, 106.58, 79.52, 73.98, 55.87, 44.74 (2C), 32.51 (2C), 28.56 (3C), 25.43 (2C), 24.36 (2C), 19.55, 18.64. HRMS (ESI): calcd. for $C_{32}H_{41}N_9O_3$ $[M+Na]^+$: 622.3230, found: 622.3228.

4.1.4. Synthesis of 2,6-dichloro-9-(tetrahydro-2H-pyran-2-yl)-9H-purine (**2d**).

2,6-dichloro-9H-purine (4.62 g, 24.03 mmol), 3,4-dihydropyran (4.38 g, 48.06 mmol) and *p*-toluenesulfonic acid (0.27 g, 1.44 mmol) were added to a 250 mL round bottom flask. DCM was used as the solvent, and the solution was reacted at room temperature for 8 h. After the reaction was completed, the reaction solution was washed with water. The organic phase was collected and dried under a vacuum to give crude the product. The crude product was then purified by silica gel column chromatography to afford 6.5 g of the target compounds as white solid with yield 99.01%. 1H NMR (400 MHz, DMSO- d_6) δ 8.95 (s, 1H), 5.74 (dd, $J = 10.8, 2.3$ Hz, 1H), 4.10 – 3.93 (m, 1H), 3.78 – 3.66 (m, 1H), 2.31 – 2.19 (m, 1H), 2.07 – 1.88 (m, 2H), 1.82 – 1.71 (m, 1H), 1.60 (p, $J = 5.9, 4.9$ Hz, 2H).

4.1.5. Synthesis of 3-(((2-chloro-9-(tetrahydro-2H-pyran-2-yl)-9H-purin-6-yl)amino)methyl)-4,6-dimethylpyridin-2(1H)-one (**3d**).

2,6-dichloro-9-(tetrahydro-2H-pyran-2-yl)-9H-purine (**2d**) (2.1 g, 7.7 mmol), 3-(aminomethyl)-4,6-dimethylpyridin-2(1H)-one (2.13 g, 13.86 mmol) and triethylamine (5.3 ml, 38.5 mmol) were added to ethanol (30 mL), and the reaction

solution was reacted under reflux at 80 ° C for 6 h. A white solid precipitated during the reaction. After the reaction was completed, the resulting suspension obtained was filtered and washed with cold ethanol (20 mL) to afford a solid product. The crude product was purified by silica gel column chromatography to afford 2.4g target compounds as white solid with yield 80.20%, mp 254-255 °C. ¹H NMR (400 MHz, DMSO-*d*₆) δ 11.52 (s, 1H), 8.33 (d, *J* = 9.3 Hz, 1H), 7.86 (t, *J* = 7.9 Hz, 1H), 5.87 (s, 1H), 5.55 (dd, *J* = 10.7 Hz, 1H), 4.45 (d, *J* = 5.3 Hz, 2H), 4.03-3.96 (m, 1H), 3.73-3.64 (m, 1H), 2.27 (s, 3H), 2.26 – 2.12 (m, 1H), 2.11 (s, 3H), 2.04 – 1.93 (m, 2H), 1.83 – 1.71 (m, 1H), 1.59 (d, *J* = 8.5 Hz, 2H). ¹³C NMR (101 MHz, Chloroform-*d*) δ 164.60, 154.82, 154.53, 151.32, 149.10, 142.76, 137.56, 121.93, 109.77, 81.52, 68.71, 36.77, 32.02, 24.79, 22.66, 19.61, 18.58. HRMS (ESI): calcd. for C₁₈H₂₁ClN₆O₂ [M+Na]⁺: 411.1313, found: 411.1310.

4.1.6. The representative procedure for the preparation of 3-(((2-substituted-9-(tetrahydro-2*H*-pyran-2-yl)-9*H*-purin-6-yl)amino)methyl)-4,6-dimethylpyridin-2(1*H*)-one derivatives (**4d1-4d8**).

4,6-dimethyl-3-(((9-(tetrahydro-2*H*-pyran-2-yl)-2-(4-(trifluoromethoxy)phenyl)-9*H*-purin-6-yl)amino)methyl)pyridin-2(1*H*)-one (**4d1**). To a stirred solution of **3d** (120 mg, 0.31 mmol) in dioxane–water mixture (16 mL/4 mL) was added (4-(trifluoromethoxy)phenyl) boronic acid pinacol ester (133.3 mg, 0.46 mmol) followed by addition of Na₂CO₃ (131.4 mg, 1.24 mmol). The solution was purged with argon for 15 minutes and then PdCl₂(dppf)·CH₂Cl₂ (22.7 mg, 0.03 mmol) was

added and the solution was again purged with argon for an additional 10 min. The reaction mixture was heated at 100 °C for 4 h. After completion (monitored by TLC), the reaction mixture was diluted with water and extracted with 10% MeOH/DCM. The combined organic layers were dried over anhydrous sodium sulphate, filtered and concentrated under reduced pressure. The crude compound was purified by column chromatography and eluted with MeOH/DCM to afford the desired compound **4d1** as a white solid. Yield: 67.10%, mp 217-219 °C. ¹H NMR (400 MHz, DMSO-*d*₆) δ 11.55 (s, 1H), 8.55 (d, *J* = 8.4 Hz, 2H), 8.36 (s, 1H), 7.47 (d, *J* = 8.6 Hz, 3H), 5.86 (s, 1H), 5.73 (dd, *J* = 10.7 Hz, 1H), 4.71 (dd, *J* = 5.3 Hz, 2H), 4.08-4.00 (m, 1H), 3.78-3.68 (m, 1H), 2.36 – 2.28 (m, 1H), 2.25 (s, 3H), 2.11 (s, 3H), 2.03-1.95 (m, 2H), 1.83-1.70 (m, 1H), 1.23 (d, *J* = 8.5 Hz, 2H). ¹³C NMR (101 MHz, DMSO-*d*₆) δ 164.17, 157.19, 154.24, 150.00, 149.63, 143.17, 139.05, 137.80, 129.94 (2C), 122.49, 120.47 (2C), 108.65, 107.56, 81.54, 68.42, 56.81, 31.13, 24.95, 22.94, 19.62, 18.65. HRMS (ESI): calcd. for C₂₅H₂₅F₃N₆O₃ [M+H]⁺: 515.2018, found: 515.2014.

3-(((2-(2-fluorophenyl)-9-(tetrahydro-2*H*-pyran-2-yl)-9*H*-purin-6-yl)amino)methyl)-4,6-dimethylpyridin-2(1*H*)-one (**4d2**). White solid, yield: 41.76%, mp 233-235 °C. ¹H NMR (400 MHz, DMSO-*d*₆) δ 11.55 (s, 1H), 8.37 (s, 1H), 7.99 (t, *J* = 7.9 Hz, 1H), 7.49 (d, *J* = 7.4 Hz, 1H), 7.36 (s, 1H), 7.30 (d, *J* = 8.0 Hz, 2H), 5.85 (s, 1H), 5.67 (d, *J* = 10.9 Hz, 1H), 4.62 (d, *J* = 5.3 Hz, 2H), 4.03-3.96 (m, 1H), 3.76 – 3.67 (m, 1H), 2.35-2.24 (m, 1H), 2.21 (d, *J* = 2.5 Hz, 3H), 2.11 (d, *J* = 2.3 Hz, 3H), 2.04 – 1.93 (m, 2H), 1.83 – 1.71 (m, 1H), 1.59 (d, *J* = 8.5 Hz, 2H). ¹³C NMR (101 MHz,

Chloroform-*d*) δ 165.45, 162.28, 159.75, 157.57, 154.32, 150.60, 143.12, 137.68, 131.97 (d, $J = 2.2$ Hz), 130.44 (d, $J = 8.5$ Hz), 128.21, 123.66 (d, $J = 3.8$ Hz), 122.52, 116.67, 116.45, 109.59, 81.60, 68.65, 32.05, 29.70, 25.00, 22.83, 19.57, 18.86. HRMS (ESI): calcd. for $C_{24}H_{25}FN_6O_2$ $[M+H]^+$: 449.2101, found: 449.2102.

4,6-dimethyl-3-(((2-(4-morpholinophenyl)-9-(tetrahydro-2*H*-pyran-2-yl)-9*H*-purin-6-yl)amino)methyl)pyridin-2(1*H*)-one (**4d3**). Brown solid, yield: 57.06%, mp 185-187 °C. 1H NMR (400 MHz, DMSO-*d*₆) δ 11.55 (s, 1H), 8.33 (s, 1H), 8.07 (s, 1H), 7.92 (d, $J = 7.6$ Hz, 1H), 7.34 (t, $J = 7.9$ Hz, 1H), 7.26 (s, 1H), 7.05 (dd, $J = 8.2, 2.5$ Hz, 1H), 5.86 (s, 1H), 5.78 – 5.69 (m, 1H), 4.73 (d, $J = 5.3$ Hz, 2H), 4.06-3.98 (m, 1H), 3.79 (t, $J = 4.8$ Hz, 4H), 3.76-3.68 (m, 1H), 3.38-3.32 (1H), 3.20 (t, $J = 4.8$ Hz, 4H), 2.29 (s, 3H), 2.11 (s, 3H), 2.04 – 1.93 (m, 2H), 1.83 – 1.71 (m, 1H), 1.59 (d, $J = 8.5$ Hz, 2H). ^{13}C NMR (101 MHz, Chloroform-*d*) δ 164.76, 159.62, 154.09, 151.27, 150.76, 142.78, 139.87, 137.65, 128.91 (2C), 122.74, 120.61, 117.48, 115.83 (2C), 109.70, 81.47, 68.65, 66.97 (2C), 49.72 (2C), 31.90, 29.63, 24.92, 22.82, 19.78, 18.56. HRMS (ESI): calcd. for $C_{28}H_{33}N_7O_3$ $[M+Na]^+$: 538.2543, found: 538.2549.

4,6-dimethyl-3-(((2-(3-morpholinophenyl)-9-(tetrahydro-2*H*-pyran-2-yl)-9*H*-purin-6-yl)amino)methyl)pyridin-2(1*H*)-one (**4d4**). Brown solid, yield: 81.87%, mp 168-170 °C. 1H NMR (400 MHz, DMSO-*d*₆) δ 11.56 (s, 1H), 8.33 (s, 1H), 8.06 (s, 1H), 7.92 (d, $J = 7.7$ Hz, 1H), 7.34 (t, $J = 7.9$ Hz, 1H), 7.27 (s, 1H), 7.06 (dd, $J = 8.1, 2.6$ Hz, 1H), 5.86 (s, 1H), 5.73 (dd, $J = 10.8, 2.1$ Hz, 1H), 4.73 (d, $J = 5.3$ Hz, 2H),

4.03-3.96 (m, 1H), 3.79 (t, $J = 4.8$ Hz, 4H), 3.76 – 3.67 (m, 1H), 3.20 (t, $J = 4.8$ Hz, 4H), 2.347-3.31(m, 1H), 2.29 (s, 3H), 2.11 (s, 3H), 2.04 – 1.93 (m, 2H), 1.83 – 1.71 (m, 1H), 1.59 (d, $J = 8.5$ Hz, 2H). ^{13}C NMR (101 MHz, Chloroform- d) δ 164.73, 159.61, 154.09, 151.28, 150.73, 142.69, 139.89, 137.63, 128.91, 122.79, 120.60, 118.17, 117.46, 115.83, 109.67, 81.47, 68.65, 66.98 (2C), 49.73 (2C), 31.92, 24.93, 22.84, 19.79, 18.59. HRMS (ESI): calcd. for $\text{C}_{28}\text{H}_{33}\text{N}_7\text{O}_3$ $[\text{M}+\text{H}]^+$: 516.2723, found: 516.2715.

4,6-dimethyl-3-(((2-(4-(morpholinomethyl)phenyl)-9-(tetrahydro-2H-pyran-2-yl)-9H-purin-6-yl)amino)methyl)pyridin-2(1H)-one (**4d5**). Off-white solid, yield: 50.39%, mp 226-228 °C. ^1H NMR (400 MHz, Chloroform- d) δ 11.91 (s, 1H), 8.44 (d, $J = 7.9$ Hz, 2H), 7.91 (s, 1H), 7.42 (d, $J = 7.9$ Hz, 2H), 6.78 (d, $J = 8.4$ Hz, 1H), 5.87 (s, 1H), 5.79 (dd, $J = 10.1, 2.8$ Hz, 1H), 4.95 (d, $J = 5.3$ Hz, 2H), 4.19-4.12 (m, 1H), 3.84-3.76 (m, 1H), 3.77 – 3.71 (m, 4H), 3.58 (s, 2H), 2.49 (s, 4H), 2.40 (s, 3H), 2.31 (s, 3H), 2.17-2.03 (m, 2H), 1.85-1.75 (m, 1H), 1.70-1.58 (m, 2H). ^{13}C NMR (101 MHz, Chloroform- d) δ 165.33, 159.15, 154.38, 150.39, 143.14, 139.02, 138.26, 137.48, 129.06 (2C), 128.21 (2C), 122.68, 115.33, 109.52, 81.58, 77.24, 68.69, 67.01 (2C), 63.29, 53.64 (2C), 31.98, 25.03, 22.95, 19.82, 18.89. HRMS (ESI): calcd. for $\text{C}_{29}\text{H}_{35}\text{N}_7\text{O}_3$ $[\text{M}+\text{H}]^+$: 530.2879, found: 530.2874.

4,6-dimethyl-3-(((2-(4-(4-methylpiperazin-1-yl)phenyl)-9-(tetrahydro-2H-pyran-2-yl)-9H-purin-6-yl)amino)methyl)pyridin-2(1H)-one (**4d6**). Brown solid, yield: 64.13%,

mp 180-182 °C. ^1H NMR (400 MHz, DMSO- d_6) δ 11.55 (s, 1H), 8.33 – 8.23 (m, 3H), 7.16 (s, 1H), 7.04 – 6.97 (m, 2H), 5.85 (s, 1H), 5.70 (dd, J = 10.9, 2.1 Hz, 1H), 4.71 (d, J = 5.3 Hz, 2H), 4.06 – 3.98 (m, 1H), 3.76-3.68 (m, 1H), 3.25 (t, J = 5.0 Hz, 4H), 2.47 (t, J = 5.0 Hz, 4H), 2.34-2.20 (m, J = 15.2 Hz, 7H), 2.04–1.93 (m, 2H), 1.83 – 1.71 (m, 1H), 1.59 (d, J = 8.7 Hz, 2H). ^{13}C NMR (101 MHz, Chloroform- d) δ 165.08, 159.45, 154.18, 152.13, 150.74, 142.94, 137.12, 130.17, 129.34 (2C), 122.78, 117.83, 114.93 (2C), 109.68, 81.47, 77.31, 68.64, 54.89 (2C), 48.36 (2C), 45.99, 31.87, 24.98, 22.90, 19.81, 18.67. HRMS (ESI): calcd. for $\text{C}_{29}\text{H}_{36}\text{N}_8\text{O}_2$ $[\text{M}+\text{H}]^+$: 529.3039, found: 529.3034.

4,6-dimethyl-3-(((2-(6-(4-methylpiperazin-1-yl)pyridin-3-yl)-9-(tetrahydro-2H-pyran-2-yl)-9H-purin-6-yl)amino)methyl)pyridin-2(1H)-one (**4d7**). Off-white solid, yield: 52.13 %, mp 223-225 °C. ^1H NMR (400 MHz, DMSO- d_6) δ 11.56 (s, 1H), 9.16 (s, 1H), 8.50 – 8.42 (m, 1H), 8.27 (s, 1H), 7.24 (s, 1H), 6.90 (d, J = 9.0 Hz, 1H), 5.86 (s, 1H), 5.70 (dd, J = 11.0, 2.1 Hz, 1H), 4.69 (d, J = 5.3 Hz, 2H), 4.06-3.98 (m, 1H), 3.76-3.68 (m, 1H), 3.59 (t, J = 5.0 Hz, 4H), 2.41 (t, J = 5.0 Hz, 4H), 2.34-2.20 (m, J = 15.2 Hz, 7H), 2.11 (s, 3H), 2.04 – 1.93 (m, 2H), 1.83 – 1.71 (m, 1H), 1.59 (d, J = 8.4 Hz, 2H). ^{13}C NMR (101 MHz, Chloroform- d) δ 165.43, 159.75, 158.07, 154.31, 150.36, 148.92, 143.16, 137.29, 137.10, 124.48, 122.66, 109.49, 105.83, 81.72, 68.65, 54.87 (2C), 46.21, 45.14 (2C), 31.71, 25.02, 22.96, 19.87, 18.87. HRMS (ESI): calcd. for $\text{C}_{28}\text{H}_{35}\text{N}_9\text{O}_2$ $[\text{M}+\text{H}]^+$: 530.2992, found: 530.2990.

tert-butyl

4-(5-(6-(((4,6-dimethyl-2-oxo-1,2-dihydropyridin-3-yl)methyl)amino)-9-(tetrahydro-2-*H*-pyran-2-yl)-9*H*-purin-2-yl)pyridin-2-yl)piperazine-1-carboxylate (**4d8**). Off-white solid, yield: 59.89%, mp 178-180 °C. ¹H NMR (400 MHz, DMSO-*d*₆) δ 11.55 (s, 1H), 8.33 (s, 1H), 8.07 (s, 1H), 7.92 (d, *J* = 7.6 Hz, 1H), 7.34 (t, *J* = 7.9 Hz, 1H), 7.26 (t, *J* = 7.9 Hz, 1H), 7.05 (dd, *J* = 8.2, 2.5 Hz, 1H), 5.86 (s, 1H), 5.78 – 5.69 (m, 1H), 4.73 (d, *J* = 5.3 Hz, 2H), 4.05-3.97 (m, 1H), 3.76-3.68 (m, 1H), 3.61 (t, *J* = 4.8 Hz, 4H), 3.46 (t, *J* = 4.8 Hz, 4H), 3.20 (d, *J* = 9.8 Hz, 1H), 2.38-2.28 (m, 1H), 2.11 (s, 3H), 2.04–1.93 (m, 2H), 1.83 – 1.71 (m, 1H), 1.59 (d, *J* = 8.7 Hz, 2H), 1.44 (s, 9H). ¹³C NMR (101 MHz, Chloroform-*d*) δ 165.46, 159.52, 157.94, 154.85, 154.32, 150.37, 148.90, 143.26, 137.42, 137.14, 124.81, 122.56, 109.49, 105.92, 81.70 (2C), 80.00 (2C), 68.64, 58.22, 45.04, 31.70, 28.44 (3C), 25.00, 22.95, 19.84, 18.83, 18.39. HRMS (ESI): calcd. for C₃₂H₄₁N₉O₄ [M+H]⁺: 616.3360, found: 616.3358.

4.1.7. The representative procedure for the preparation of 3-(((2-substituted-9-substituted-9*H*-purin-6-yl)amino)methyl)-4,6-dimethylpyridin-2(1*H*)-one derivatives (**5a-5k**).

3-(((9-isopropyl-2-(6-(piperazin-1-yl)pyridin-3-yl)-9*H*-purin-6-yl)amino)methyl)-4,6-dimethylpyridin-2(1*H*)-one (**5a**). **4a7** (122 mg, 0.21 mmol) was dissolved in DCM, trifluoroacetic acid (TFA) (156.0 μL, 2.1 mmol) was added dropwise. The resulting solution was stirred at room temperature overnight. After completion (monitored by TLC), the reaction solution was concentrated under reduced pressure.

Sodium bicarbonate (NaHCO_3) solution was added to the concentrate under stirring to adjust the pH to 8-9, and a light yellow solid precipitated. Filtered and dried to obtain the target compound. Brown solid, yield: 84.85%, mp 249-250 °C. ^1H NMR (400 MHz, $\text{DMSO}-d_6$) δ 11.54 (s, 1H), 9.14 (s, 1H), 8.44 (d, $J = 9.0$ Hz, 1H), 8.16 (s, 1H), 7.12 (t, $J = 5.7$ Hz, 1H), 6.86 (d, $J = 9.0$ Hz, 1H), 5.85 (s, 1H), 4.79 (m, $J = 6.7$ Hz, 1H), 4.69 (d, $J = 5.3$ Hz, 2H), 3.51 (t, $J = 5.0$ Hz, 4H), 2.79 (t, $J = 5.1$ Hz, 4H), 2.28 (s, 3H), 2.10 (s, 3H), 1.55 (d, $J = 6.7$ Hz, 6H). ^{13}C NMR (101 MHz, $\text{Chloroform}-d$) δ 165.42, 159.96, 157.55, 154.32, 150.29, 148.82, 143.05, 137.20, 136.96, 124.65, 122.84, 118.80, 109.47, 105.80, 58.33, 46.88, 46.37 (2C), 45.91 (2C), 22.65 (2C), 19.90, 18.88. HRMS (ESI): calcd. for $\text{C}_{25}\text{H}_{31}\text{N}_9\text{O}$ $[\text{M}+\text{H}]^+$: 474.2730 found: 474.2729.

4,6-dimethyl-3-(((9-(pentan-3-yl)-2-(6-(piperazin-1-yl)pyridin-3-yl)-9*H*-purin-6-yl)amino)methyl)pyridin-2(1*H*)-one (**5b**). Brown solid, yield: 76.15%, mp 166-167 °C. ^1H NMR (400 MHz, $\text{DMSO}-d_6$) δ 11.59 (s, 1H), 9.13 (s, 1H), 8.42 (d, $J = 8.8$ Hz, 1H), 8.11 (s, 1H), 7.14 (t, $J = 5.7$ Hz, 1H), 6.86 (d, $J = 9.0$ Hz, 1H), 5.86 (s, 1H), 4.69 (d, $J = 5.3$ Hz, 2H), 4.30 (m, $J = 4.8$ Hz, 1H), 3.51 (t, $J = 4.9$ Hz, 4H), 2.80 (t, $J = 4.9$ Hz, 4H), 2.29 (s, 3H), 2.11 (s, 3H), 2.08 – 1.89 (m, 4H), 0.72 (t, $J = 7.3$ Hz, 6H). ^{13}C NMR (101 MHz, $\text{Chloroform}-d$) δ 164.60, 159.73, 157.45, 154.00, 150.95, 150.36, 148.46, 142.58, 138.41, 137.49, 124.75, 122.80, 118.16, 109.74, 106.20, 59.43, 57.64, 45.91 (2C), 45.23 (2C), 27.54 (2C), 19.69, 18.43, 10.55 (2C). HRMS (ESI): calcd. for $\text{C}_{27}\text{H}_{35}\text{N}_9\text{O}$ $[\text{M}+\text{H}]^+$: 502.3043 found: 502.3040.

3-(((9-cyclopentyl-2-(6-(piperazin-1-yl)pyridin-3-yl)-9*H*-purin-6-yl)amino)methyl)-4,6-dimethylpyridin-2(1*H*)-one (**5c**). Brown solid, yield: 85.13%, mp 174-176 °C. ¹H NMR (400 MHz, DMSO-*d*₆) δ 11.55 (s, 1H), 9.13 (s, 1H), 8.44 (d, *J* = 8.9 Hz, 1H), 8.13 (s, 1H), 7.13 (t, *J* = 7.9 Hz, 1H), 6.86 (d, *J* = 9.0 Hz, 1H), 5.85 (s, 1H), 4.89 (m, 1H), 4.69 (d, *J* = 5.3 Hz, 2H), 3.51 (t, *J* = 4.9 Hz, 4H), 2.79 (t, *J* = 5.0 Hz, 4H), 2.28 (s, 3H), 2.23 – 2.14 (m, 2H), 2.10 (s, 3H), 2.08 – 2.00 (m, 2H), 1.98 – 1.89 (m, 2H), 1.76 – 1.69 (m, 2H). ¹³C NMR (101 MHz, Chloroform-*d*) δ 164.56, 159.77, 157.51, 154.01, 150.97, 150.04, 148.47, 142.55, 137.87, 137.47, 124.65, 122.79, 118.27, 109.75, 106.22, 57.65, 55.99, 45.96 (2C), 45.29 (2C), 32.59 (2C), 24.03 (2C), 19.68, 18.43. HRMS (ESI): calcd. for C₂₇H₃₃N₉O [M+H]⁺: 500.2886 found: 500.2888.

4,6-dimethyl-3-(((2-(4-(trifluoromethoxy)phenyl)-9*H*-purin-6-yl)amino)methyl)pyridine-2(1*H*)-one (**5d**). White solid, yield: 92.31%, mp 250-251 °C. ¹H NMR (400 MHz, DMSO-*d*₆) δ 12.88 (s, 1H), 11.56 (s, 1H), 8.52 (d, *J* = 8.7 Hz, 2H), 8.14 (s, 1H), 7.45 (d, *J* = 8.5 Hz, 2H), 7.29 (t, *J* = 5.7 Hz 1H), 5.87 (s, 1H), 4.71 (d, *J* = 5.3 Hz, 2H), 2.27 (s, 3H), 2.11 (s, 3H). ¹³C NMR (101 MHz, DMSO-*d*₆) δ 163.85, 156.60, 149.71, 149.39, 143.30, 140.85, 138.58, 130.16, 129.94 (2C), 122.61, 121.86, 121.01 (2C), 119.31, 108.04, 36.38, 19.56, 18.65. HRMS (ESI): calcd. for C₂₀H₁₇F₃N₆O₂ [M+Na]⁺: 453.1263, found: 453.1265.

3-(((2-(2-fluorophenyl)-9*H*-purin-6-yl)amino)methyl)-4,6-dimethylpyridin-2(1*H*)-one

(**5e**). White solid, yield: 94.71%, mp 277-278 °C. ^1H NMR (400 MHz, $\text{DMSO-}d_6$) δ 13.05 (s, 1H), 11.56 (s, 1H), 8.17 (s, 1H), 8.00 (t, $J = 8.1$ Hz, 1H), 7.47 (q, $J = 7.0$ Hz, 1H), 7.39 – 7.15 (m, 3H), 5.86 (s, 1H), 4.62 (d, $J = 5.3$ Hz, 2H), 2.23 (s, 3H), 2.11 (s, 3H). ^{13}C NMR (101 MHz, $\text{DMSO-}d_6$) δ 163.87, 161.92, 159.42, 156.42, 149.40, 143.30, 140.75, 132.15 (d, $J = 2.3$ Hz), 131.11 (d, $J = 8.2$ Hz), 128.40, 128.30, 124.42 (d, $J = 3.6$ Hz), 122.55, 116.99, 116.76, 108.08, 36.58, 19.34, 18.63. HRMS (ESI): calcd. for $\text{C}_{19}\text{H}_{17}\text{FN}_6\text{O}$ $[\text{M}+\text{H}]^+$: 365.1526 found: 365.1527.

4,6-dimethyl-3-(((2-(4-morpholinophenyl)-9H-purin-6-yl)amino)methyl)pyridin-2(1H)-one (**5f**). White solid, yield: 79.89%, mp 266-267 °C. ^1H NMR (400 MHz, $\text{DMSO-}d_6$) δ 13.05 (s, 1H), 11.61 (s, 1H), 8.16 (s, 1H), 8.00 (s, 1H), 7.88 (d, $J = 7.6$ Hz, 1H), 7.34 (t, $J = 8.0$ Hz, 2H), 7.06 (d, $J = 8.2$ Hz, 1H), 5.88 (s, 1H), 4.73 (d, $J = 5.3$ Hz, 2H), 3.79 (t, $J = 4.6$ Hz, 4H), 3.19 (t, $J = 5.0$ Hz, 4H), 2.30 (s, 3H), 2.12 (s, 3H). ^{13}C NMR (101 MHz, $\text{Chloroform-}d$) δ 164.48, 159.75, 151.27, 151.17, 142.77, 139.76, 138.42, 129.01 (2C), 122.64, 120.26, 117.34, 115.64 (2C), 110.48, 110.12, 66.90 (2C), 49.53 (2C), 29.61, 19.75, 18.46. HRMS (ESI): calcd. for $\text{C}_{23}\text{H}_{25}\text{N}_7\text{O}_2$ $[\text{M}+\text{H}]^+$: 432.2148 found: 432.2148.

4,6-dimethyl-3-(((2-(3-morpholinophenyl)-9H-purin-6-yl)amino)methyl)pyridin-2(1H)-one (**5g**). White solid, yield: 85.18%, mp 255-256 °C. ^1H NMR (400 MHz, $\text{DMSO-}d_6$) δ 13.04 (s, 1H), 11.60 (s, 1H), 8.15 (s, 1H), 8.00 (s, 1H), 7.88 (d, $J = 7.5$ Hz, 1H), 7.33 (t, $J = 7.9$ Hz, 2H), 7.06 (d, $J = 8.3$ Hz, 1H), 5.88 (s, 1H), 4.73 (d, $J =$

5.3 Hz, 2H), 3.79 (t, $J = 4.7$ Hz, 4H), 3.18 (t, $J = 4.8$ Hz, 4H), 2.30 (s, 3H), 2.12 (s, 3H). ^{13}C NMR (101 MHz, DMSO- d_6) δ 163.88, 157.77, 152.98, 151.59, 149.49, 143.55, 140.88, 139.07, 129.35, 128.78, 122.69, 122.57, 119.52, 117.39, 114.68, 108.29, 66.63 (2C), 49.13 (2C), 29.48, 19.59, 18.65. HRMS (ESI): calcd. for $\text{C}_{23}\text{H}_{25}\text{N}_7\text{O}_2$ $[\text{M}+\text{H}]^+$: 432.2148 found: 432.2143.

4,6-dimethyl-3-(((2-(4-(morpholinomethyl)phenyl)-9*H*-purin-6-yl)amino)methyl)pyridin-2(1*H*)-one (**5h**). White solid, yield: 74.82%, mp 198-199 °C. ^1H NMR (400 MHz, DMSO- d_6) δ 12.95 (s, 1H), 11.57 (s, 1H), 8.37 (d, $J = 8.3$ Hz, 2H), 8.10 (s, 1H), 7.40 (d, $J = 7.8$ Hz, 2H), 7.18 (t, $J = 5.7$ Hz, 1H), 5.87 (s, 1H), 4.71 (d, $J = 5.3$ Hz, 2H), 3.59 (t, $J = 4.5$ Hz, 4H), 3.52 (s, 2H), 2.39 (t, $J = 4.5$ Hz, 4H), 2.28 (s, 3H), 2.11 (s, 3H). ^{13}C NMR (101 MHz, Chloroform- d) δ 168.45, 163.36, 155.28, 149.78, 146.65, 142.47, 142.05, 133.26 (2C), 132.06 (2C), 126.57, 119.17, 113.87, 70.67 (2C), 67.06, 57.37 (2C), 33.53, 23.58, 22.32. HRMS (ESI): calcd. for $\text{C}_{24}\text{H}_{27}\text{N}_7\text{O}_2$ $[\text{M}+\text{H}]^+$: 446.2304 found: 446.2299.

4,6-dimethyl-3-(((2-(4-(4-methylpiperazin-1-yl)phenyl)-9*H*-purin-6-yl)amino)methyl)pyridin-2(1*H*)-one (**5i**). White solid, yield: 95.09%, mp 265-266 °C. ^1H NMR (400 MHz, DMSO- d_6) δ 12.83 (s, 1H), 11.56 (s, 1H), 8.27 (d, $J = 8.4$ Hz, 2H), 8.02 (s, 1H), 7.70 – 6.62 (m, 3H), 5.86 (s, 1H), 4.70 (d, $J = 5.3$ Hz, 2H), 3.27 – 3.10 (m, 4H), 2.56 (s, 4H), 2.29 (d, $J = 8.2$ Hz, 6H), 2.11 (s, 3H). ^{13}C NMR (101 MHz, Chloroform- d) δ 164.46, 159.48, 153.52, 151.82, 151.24, 142.65, 138.17, 129.93 (2C),

129.21, 122.66, 115.02 (2C), 109.98, 54.55 (2C), 47.81 (2C), 45.45, 29.57, 19.69, 18.41. HRMS (ESI): calcd. for $C_{24}H_{28}N_8O$ $[M+H]^+$: 445.2464 found: 445.2462.

4,6-dimethyl-3-(((2-(6-(4-methylpiperazin-1-yl)pyridin-3-yl)-9*H*-purin-6-yl)amino)methyl)pyridin-2(1*H*)-one (**5j**). White solid, yield: 89.02%, mp 285-286 °C. 1H NMR (400 MHz, DMSO-*d*₆) δ 12.76 (s, 1H), 11.57 (s, 1H), 9.11 (s, 1H), 8.43 (d, J = 9.2 Hz, 1H), 8.05 (s, 1H), 7.13 (t, J = 8.1 Hz, 1H), 6.89 (d, J = 9.0 Hz, 1H), 5.86 (s, 1H), 4.70 (d, J = 5.3 Hz, 2H), 3.58 (t, J = 4.6 Hz, 4H), 2.41 (t, J = 5.0 Hz, 4H), 2.28 (s, 3H), 2.23 (s, 3H), 2.11 (s, 3H). ^{13}C NMR (101 MHz, Chloroform-*d*) δ 164.55, 159.56, 158.08, 151.08, 148.43, 142.64, 137.35, 124.27, 122.65, 109.90, 106.27, 54.59 (2C), 45.83, 44.78 (2C), 29.59, 19.71, 18.47. HRMS (ESI): calcd. for $C_{23}H_{27}N_9O$ $[M+H]^+$: 446.2417 found: 446.2418.

4,6-dimethyl-3-(((2-(6-(piperazin-1-yl)pyridin-3-yl)-9*H*-purin-6-yl)amino)methyl)pyridin-2(1*H*)-one (**5k**). White solid, yield: 84.52%, mp 241-243 °C. 1H NMR (400 MHz, DMSO-*d*₆) δ 11.57 (s, 1H), 9.11 (s, 1H), 8.42 (d, J = 9.2 Hz, 1H), 8.05 (s, 1H), 7.12 (t, J = 5.7 Hz 1H), 6.85 (d, J = 9.0 Hz, 1H), 5.86 (s, 1H), 4.69 (d, J = 5.3 Hz, 2H), 3.51 (t, J = 4.9 Hz, 4H), 2.80 (t, J = 4.8 Hz, 4H), 2.28 (s, 3H), 2.11 (s, 3H). ^{13}C NMR (101 MHz, Chloroform-*d*) δ 168.41, 163.77, 162.01, 155.40, 152.13, 146.82, 141.45, 128.33, 126.66, 113.81, 110.41, 61.24, 49.72 (2C), 49.04 (2C), 23.33, 21.97. HRMS (ESI): calcd. for $C_{22}H_{25}N_9O$ $[M+H]^+$: 432.2260 found: 432.2255.

4.1.8. Synthesis of 6-chloro-9-cyclopentyl-9*H*-purine (**2e**).

6-dichloro-9*H*-purine (2.0 g, 12.94 mmol), and potassium carbonate (K_2CO_3) (5.36 g, 38.82 mmol) were dissolved in 20 ml anhydrous DMSO. Bromocyclopentane (6.9 mL, 64.7 mmol) was added dropwise at 15 °C. The reaction mixture was stirred at 15 °C overnight. Upon completion of the reaction, the reaction solution was poured into ice water, and a white solid precipitated. The solution was filtered and dried under a vacuum to give 2.4 g of white solid. Yield: 83.3%. 1H NMR (400 MHz, $DMSO-d_6$) δ 8.78 (s, 1H), 8.77 (s, 1H), 5.00 (p, $J = 7.5$ Hz, 1H), 2.27-2.17 (m, 2H), 2.12-2.04 (m, 2H), 1.97-1.85 (m, 2H), 1.77-1.69 (m, 2H).

4.1.9. Synthesis of

3-(((9-cyclopentyl-9*H*-purin-6-yl)amino)methyl)-4,6-dimethylpyridin-2(1*H*)-one (**3e**).

6-chloro-9-cyclopentyl-9*H*-purine (**2e**) (200 mg, 0.90 mmol), 3-(aminomethyl)-4,6-dimethylpyridin-2(1*H*)-one (174.5 mg, 1.17 mmol) and triethylamine (624 μ l, 4.50 mmol) were added to ethanol (5 mL), and the reaction solution was reacted under reflux at 80 °C for 6 h. A white solid precipitated during the reaction. After the reaction was completed, the resulting suspension obtained was filtered and washed with cold ethanol (10 mL) to afford a solid product. The crude product was purified by silica gel column chromatography to afford 102 mg target compounds as white solid with yield 33.48%, mp 179-181 °C. 1H NMR (400 MHz, $DMSO-d_6$) δ 11.52 (s, 1H), 8.24 (s, 1H), 8.19 (s, 1H), 7.15 (t, $J = 5.6$ Hz, 1H), 5.86 (s, 1H), 4.83 (p, $J = 7.6$ Hz, 1H), 4.55 (s, 2H), 2.25 (s, 3H), 2.18 – 2.08 (m, 5H), 2.04 –

1.93 (m, 2H), 1.92 – 1.82 (m, 2H), 1.74 – 1.63 (m, 2H). ^{13}C NMR (101 MHz, Chloroform-*d*) δ 165.49, 154.74, 152.71, 150.51, 149.12, 143.43, 137.48, 122.09, 120.23, 109.49, 55.74, 36.64, 32.71(2C), 23.76 (2C), 19.64, 18.77. HRMS (ESI): calcd. for $\text{C}_{18}\text{H}_{22}\text{N}_6\text{O}$ $[\text{M}+\text{H}]^+$: 339.1933 found: 339.1932.

4.2. Molecular Modelling

The 3D structure of the tubulin was downloaded from the PDB (<http://www.rcsb.org/>, PDB code 402B). The protein was prepared with discovery studio 3.1. Molecule SKLB0533 was built with ChemBio3D and optimized at molecular mechanical level. The structure of colchicine was directly extracted from the crystal structure composed of tubulin and colchicine. Then SKLB0533 was docked to the binding site of tubulin by employing a protein-ligand docking program GOLD5.2. Scoring function GOLDScore was used for exhaustive searching, solid body optimizing, and interaction scoring.

4.3. *In vitro* tubulin polymerization assay

The fluorescence-based *in vitro* tubulin polymerization assay was performed using a Tubulin Polymerization Assay Kit (BK011P, Cytoskeleton, USA) according to the manual. First, a 96-well plate was incubated with 5 μL of compounds at various concentrations at 37 $^{\circ}\text{C}$ for 1 min. Then 50 μL of the tubulin reaction mix was added. The increase in fluorescence was immediately monitored by excitation at 355 nm and emission at 460 nm in a multimode reader.

4.4. Cell culture

All of the cell lines used in our study were purchased from the American Type Culture Collection (ATCC). The cells were maintained in DMEM or RPMI 1640 medium supplemented with 10% foetal bovine serum (FBS) and 1% Penicillin-Streptomycin under humidified conditions with 5% CO₂ at 37 °C.

4.5. Cell proliferation and colony formation assay

The effect of compounds on cell proliferation were assessed using the MTT assay and colony formation assays. Cells were seeded ($2\sim5\times10^3$ cells per well) in 96-well plates and incubated for 24 h and then treated with different doses of the compounds. After 72 h, 20 µL of MTT (5 mg/ml) was added to each well and incubated for 2.5 h at 37 °C. Then the medium was removed and 150 µL DMSO was added to dissolve the formazan crystal. The absorbance of each well was determined by a Spectra Max M5 microplate spectrophotometer (Molecular Devices) at a wavelength of 570 nm. The IC₅₀ values were calculated using the GraphPad Prism 8 software. For the colony formation assay, cells (600 cells per well) were seeded in 6-well plates and incubated for 24 h before being then treated with different doses of the compounds for 14 days. The cells were subsequently fixed with 4% paraformaldehyde and stained with 0.05% crystal violet. Finally, cells were visualized using an inverted microscope.

4.6. Cell cycle and apoptosis analysis by flow cytometry (FCM)

For cell cycle analysis, cells were treated with SKLB0533 for 24 h, then, cells were harvested, fixed with 75% ethanol for 2 h and stained with a PI staining solution for 10 min in the dark for analysis.

For analysis of apoptosis analysis, cells were treated with SKLB0533 for 48 h, then the cells were harvested and stained by Annexin V-Fluorescein isothiocyanate (FITC) apoptosis detection kit (Roche, Indianapolis, IN, USA) according to the manufacturer's protocol. The data were analyzed by NovoExpress 1.1.2 Software.

4.7. Western blotting analysis

Cells were treated with SKLB0533 for the indicated time and lysed in RIPA buffer containing cocktail (1/1000) and phosphatase inhibitors for 1 h. Then, cell lysates were centrifuged at 13000 rpm at 4°C for 30 min, the supernatant was harvested and the protein concentration was determined by the BCA method. The equal protein samples were separated on SDS-PAGE gel and transferred onto nitrocellulose (NC) filter membranes. Then the membranes were incubated with relevant primary antibody and secondary antibody. Specific protein bands were detected via chemiluminescence.

4.8. Immunofluorescence (IF) analysis

The IF analysis was conducted according to standard protocols with minor modifications due to antibody optimization.

4.9. *In vivo* xenograft models study

All mice used in this study were purchased from Beijing HFK Bioscience Co.Ltd. To investigate the antitumor activity of SKLB0533 *in vivo*, 100 μ L tumour cell suspension containing 1×10^7 cells were subcutaneously injected into the right-flanks of BALB/C nude mice (6 weeks). When average volume of the tumors reached to about 100 mm³, the mice were randomly divided into 4 groups (7 mice per group) randomly. Indicated doses of SKLB0533 and control were administered once daily by oral dosing for 28 days. Tumour volumes and body weight were measured every 3 days. Tumour volumes were calculated according to the following formula: tumor volume (mm³) = $0.52 \times a \times b^2$ (a represents length and b represents width). The TGI values were calculated with the following formula: $TGI = [1 - (T_{28} - T_0) / (C_{28} - C_0)] \times 100\%$, T_0 and T_{28} represent average tumour volume on day 0 and day 28 after treatment in SKLB0533- and capecitabine-treated group, C_0 and C_{28} represent the average tumour volume on day 0 and day 28, respectively, after treatment in the control group.

Conflicts of interest

The authors declare no conflict of interest about this article.

Acknowledgments

We are grateful for Shuhui Xu and Lihua Zhou of State Key Laboratory of Biotherapy (Sichuan University) for NMR measurements and Professor Lijuan Chen's team of State Key Laboratory of Biotherapy (Sichuan University) for HRMS

measurements. This work was supported by Sichuan Provincial Science and Technology Program for Key Research and Development, China (No.2018SZ0007).

Supplementary data

Supplementary data related to this article can be found at <http://dx.doi.org/10.xxxx/j.ejmech.2019.xx.xxx>

References

- [1] F. Bray, J. Ferlay, I. Soerjomataram, R.L. Siegel, L.A. Torre, and A. Jemal, Global cancer statistics 2018: GLOBOCAN estimates of incidence and mortality worldwide for 36 cancers in 185 countries. *CA Cancer J. Clin.* 68(2018)394-424.
- [2] K.D. Miller, L. Nogueira, A.B. Mariotto, J.H. Rowland, K.R. Yabroff, C.M. Alfano, A. Jemal, J.L. Kramer, and R.L. Siegel, Cancer treatment and survivorship statistics, 2019. *CA Cancer J. Clin.* 2019.
- [3] R.L. Siegel, K.D. Miller, and A. Jemal, Colorectal Cancer Mortality Rates in Adults Aged 20 to 54 Years in the United States, 1970-2014. *JAMA* 318(2017)572-574.
- [4] M. Kavallaris, Microtubules and resistance to tubulin-binding agents. *Nat. Rev. Cancer* 10(2010)194-204.
- [5] M.A. Jordan and L. Wilson, Microtubules as a target for anticancer drugs. *Nat. Rev. Cancer* 4(2004)253-265.
- [6] A.E. Protá, K. Bargsten, D. Zurwerra, J.J. Field, J.F. Diaz, K.H. Altmann, and

- M.O. Steinmetz, Molecular mechanism of action of microtubule-stabilizing anticancer agents. *Science* 339(2013)587-590.
- [7] L.J. Leandro-Garcia, S. Leskela, I. Landa, C. Montero-Conde, E. Lopez-Jimenez, R. Leton, A. Cascon, M. Robledo, and C. Rodriguez-Antona, Tumoral and tissue-specific expression of the major human beta-tubulin isotypes. *Cytoskeleton* 67(2010)214-223.
- [8] J. Kilner, B.M. Corfe, M.T. McAuley, and S.J. Wilkinson, A deterministic oscillatory model of microtubule growth and shrinkage for differential actions of short chain fatty acids. *Mol. Biosyst.* 12(2016)93-101.
- [9] F. Naaz, M.R. Haider, S. Shafi, and M.S. Yar, Anti-tubulin agents of natural origin: Targeting taxol, vinca, and colchicine binding domains. *Eur. J. Med. Chem.* 171(2019)310-331.
- [10] P. Giannakakou, D. Sackett, and T. Fojo, Tubulin/microtubules: still a promising target for new chemotherapeutic agents. *J. Natl. Cancer Inst.* 92(2000)182-183.
- [11] R. Romagnoli, M. Kimatrai Salvador, S. Schiaffino Ortega, P.G. Baraldi, P. Oliva, S. Baraldi, L.C. Lopez-Cara, A. Brancale, S. Ferla, E. Hamel, J. Balzarini, S. Liekens, E. Mattiuzzo, G. Basso, and G. Viola, 2-Alkoxycarbonyl-3-arylamino-5-substituted thiophenes as a novel class of antimicrotubule agents: Design, synthesis, cell growth and tubulin polymerization inhibition. *Eur. J. Med. Chem.* 143(2018)683-698.
- [12] Y.N. Cao, L.L. Zheng, D. Wang, X.X. Liang, F. Gao, and X.L. Zhou, Recent advances in microtubule-stabilizing agents. *Eur. J. Med. Chem.*

143(2018)806-828.

- [13] J. Konner, R.N. Grisham, J. Park, O.A. O'Connor, G. Cropp, R. Johnson, A.L. Hannah, M.L. Hensley, P. Sabbatini, S. Mironov, S. Danishefsky, D. Hyman, D.R. Spriggs, J. Dupont, and C. Aghajanian, Phase I clinical, pharmacokinetic, and pharmacodynamic study of KOS-862 (Epothilone D) in patients with advanced solid tumors and lymphoma. *Invest. New. Drugs* 30(2012)2294-2302.
- [14] P.A. Wender, S.G. Hegde, R.D. Hubbard, L. Zhang, and S.L. Mooberry, Synthesis and biological evaluation of (-)-laulimalide analogues. *Org. Lett.* 5(2003)3507-3509.
- [15] S.A. Hill, S.J. Lonergan, J. Denekamp, and D.J. Chaplin, Vinca alkaloids: anti-vascular effects in a murine tumour. *Eur. J. Cancer* 29A(1993)1320-1324.
- [16] K. Aoki, K. Watanabe, M. Sato, M. Ikekita, T. Hakamatsuka, and T. Oikawa, Effects of rhizoxin, a microbial angiogenesis inhibitor, on angiogenic endothelial cell functions. *Eur. J. Pharmacol.* 459(2003)131-138.
- [17] E. Bonfoco, S. Ceccatelli, L. Manzo, and P. Nicotera, Colchicine induces apoptosis in cerebellar granule cells. *Exp. Cell Res.* 218(1995)189-200.
- [18] G.R. Pettit, S.B. Singh, E. Hamel, C.M. Lin, D.S. Alberts, and D. Garcia-Kendall, Isolation and structure of the strong cell growth and tubulin inhibitor combretastatin A-4. *Experientia* 45(1989)209-211.
- [19] J.Y. Blay, Z. Papai, A.W. Tolcher, A. Italiano, D. Cupissol, A. Lopez-Pousa, S.P. Chawla, E. Bompas, N. Babovic, N. Penel, N. Isambert, A.P. Staddon, E. Saada-Bouazid, A. Santoro, F.A. Franke, P. Cohen, S. Le-Guenec, and G.D.

- Demetri, Ombrabulin plus cisplatin versus placebo plus cisplatin in patients with advanced soft-tissue sarcomas after failure of anthracycline and ifosfamide chemotherapy: a randomised, double-blind, placebo-controlled, phase 3 trial. *Lancet Oncol.* 16(2015)531-540.
- [20] H. Chen, Y. Li, C. Sheng, Z. Lv, G. Dong, T. Wang, J. Liu, M. Zhang, L. Li, T. Zhang, D. Geng, C. Niu, and K. Li, Design and synthesis of cyclopropylamide analogues of combretastatin-A4 as novel microtubule-stabilizing agents. *J. Med. Chem.* 56(2013)685-699.
- [21] J. Seligmann and C. Twelves, Tubulin: an example of targeted chemotherapy. *Future Med. Chem.* 5(2013)339-352.
- [22] A. Canta, A. Chiorazzi, and G. Cavaletti, Tubulin: a target for antineoplastic drugs into the cancer cells but also in the peripheral nervous system. *Curr. Med. Chem.* 16(2009)1315-1324.
- [23] M.P. Tantak, L. Klingler, V. Arun, A. Kumar, R. Sadana, and D. Kumar, Design and synthesis of bis(indolyl)ketohydrazide-hydrazones: Identification of potent and selective novel tubulin inhibitors. *Eur. J. Med. Chem.* 136(2017)184-194.
- [24] M. Zhai, S. Liu, M. Gao, L. Wang, J. Sun, J. Du, Q. Guan, K. Bao, D. Zuo, Y. Wu, and W. Zhang, 3,5-Diaryl-1H-pyrazolo[3,4-b]pyridines as potent tubulin polymerization inhibitors: Rational design, synthesis and biological evaluation. *Eur. J. Med. Chem.* 168(2019)426-435.
- [25] Y. Zhou, W. Yan, D. Cao, M. Shao, D. Li, F. Wang, Z. Yang, Y. Chen, L. He, T. Wang, M. Shen, and L. Chen, Design, synthesis and biological evaluation of

- 4-anilinoquinoline derivatives as novel potent tubulin depolymerization agents. Eur. J. Med. Chem. 138(2017)1114-1125.
- [26] S. Kasibhatla, V. Baichwal, S.X. Cai, B. Roth, I. Skvortsova, S. Skvortsov, P. Lukas, N.M. English, N. Sirisoma, J. Drewe, A. Pervin, B. Tseng, R.O. Carlson, and C.M. Pleiman, MPC-6827: a small-molecule inhibitor of microtubule formation that is not a substrate for multidrug resistance pumps. Cancer Res. 67(2007)5865-5871.
- [27] A. Gangjee, Y. Zhao, S. Raghavan, C.C. Rohena, S.L. Mooberry, and E. Hamel, Structure-activity relationship and in vitro and in vivo evaluation of the potent cytotoxic anti-microtubule agent N-(4-methoxyphenyl)-N,2,6-trimethyl-6,7-dihydro-5H-cyclopenta[d]pyrimidin-4-amine chloride and its analogues as antitumor agents. J. Med. Chem. 56(2013)6829-6844.
- [28] Y.T. Chang, S.M. Wignall, G.R. Rosania, N.S. Gray, S.R. Hanson, A.I. Su, J. Merlie, Jr., H.S. Moon, S.B. Sangankar, O. Perez, R. Heald, and P.G. Schultz, Synthesis and biological evaluation of myoseverin derivatives: microtubule assembly inhibitors. J. Med. Chem. 44(2001)4497-4500.
- [29] V. Krystof, D. Moravcova, M. Paprskarova, P. Barbier, V. Peyrot, A. Hlobilkova, L. Havlicek, and M. Strnad, Synthesis and biological activity of 8-azapurine and pyrazolo[4,3-d]pyrimidine analogues of myoseverin. Eur. J. Med. Chem. 41(2006)1405-1411.
- [30] A.E. Prota, F. Danel, F. Bachmann, K. Bargsten, R.M. Buey, J. Pohlmann, S.

- Reinelt, H. Lane, and M.O. Steinmetz, The novel microtubule-destabilizing drug BAL27862 binds to the colchicine site of tubulin with distinct effects on microtubule organization. *J. Mol. Biol.* 426(2014)1848-1860.
- [31]N. Masurier, E. Debiton, A. Jacquemet, A. Bussiere, J.M. Chezal, A. Ollivier, D. Tetegan, M. Andaloussi, M.J. Galmier, J. Lacroix, D. Canitrot, J.C. Teulade, R.C. Gaudreault, O. Chavignon, and E. Moreau, Imidazonaphthyridine systems (part 2): Functionalization of the phenyl ring linked to the pyridine pharmacophore and its replacement by a pyridinone ring produces intriguing differences in cytotoxic activity. *Eur. J. Med. Chem.* 52(2012)137-150.
- [32]N. Oumata, K. Bettayeb, Y. Ferandin, L. Demange, A. Lopez-Giral, M.L. Goddard, V. Myrianthopoulos, E. Mikros, M. Flajolet, P. Greengard, L. Meijer, and H. Galons, Roscovitine-derived, dual-specificity inhibitors of cyclin-dependent kinases and casein kinases 1. *J. Med. Chem.* 51(2008)5229-5242.
- [33]K.W. Kuntz, J.E. Campbell, H. Keilhack, R.M. Pollock, S.K. Knutson, M. Porter-Scott, V.M. Richon, C.J. Sneeringer, T.J. Wigle, C.J. Allain, C.R. Majer, M.P. Moyer, R.A. Copeland, and R. Chesworth, The Importance of Being Me: Magic Methyls, Methyltransferase Inhibitors, and the Discovery of Tazemetostat. *J. Med. Chem.* 59(2016)1556-1564.
- [34]M. Legraverend and D.S. Grierson, The purines: potent and versatile small molecule inhibitors and modulators of key biological targets. *Bioorg. Med. Chem.* 14(2006)3987-4006.

- [35] F.I. Raynaud, P.M. Fischer, B.P. Nutley, P.M. Goddard, D.P. Lane, and P. Workman, Cassette dosing pharmacokinetics of a library of 2,6,9-trisubstituted purine cyclin-dependent kinase 2 inhibitors prepared by parallel synthesis. *Mol. Cancer Ther.* 3(2004)353-362.
- [36] Y. Wang, C.A. Metcalf, 3rd, W.C. Shakespeare, R. Sundaramoorthi, T.P. Keenan, R.S. Bohacek, M.R. van Schravendijk, S.M. Violette, S.S. Narula, D.C. Dalgarno, C. Haraldson, J. Keats, S. Liou, U. Mani, S. Pradeepan, M. Ram, S. Adams, M. Weigele, and T.K. Sawyer, Bone-targeted 2,6,9-trisubstituted purines: novel inhibitors of Src tyrosine kinase for the treatment of bone diseases. *Bioorg. Med. Chem. Lett.* 13(2003)3067-3070.
- [37] I. Giorgi, G. Biagi, O. Livi, M. Leonardi, V. Scartoni, and D. Pietra, Synthesis of new 2-phenyladenines and 2-phenylpteridines and biological evaluation as adenosine receptor ligands. *Arch. Pharm.* 340(2007)81-87.
- [38] H.U. Kaniskan, M.L. Martini, and J. Jin, Inhibitors of Protein Methyltransferases and Demethylases. *Chem. Rev.* 118(2018)989-1068.
- [39] P.K. Singh, Histone methyl transferases: A class of epigenetic opportunities to counter uncontrolled cell proliferation. *Eur. J. Med. Chem.* 166(2019)351-368.
- [40] S.K. Verma, X. Tian, L.V. LaFrance, C. Duquenne, D.P. Suarez, K.A. Newlander, S.P. Romeril, J.L. Burgess, S.W. Grant, J.A. Brackley, A.P. Graves, D.A. Scherzer, A. Shu, C. Thompson, H.M. Ott, G.S. Aller, C.A. Machutta, E. Diaz, Y. Jiang, N.W. Johnson, S.D. Knight, R.G. Kruger, M.T. McCabe, D. Dhanak, P.J. Tummino, C.L. Creasy, and W.H. Miller, Identification of Potent, Selective,

Cell-Active Inhibitors of the Histone Lysine Methyltransferase EZH2. ACS Med.

Chem. Lett. 3(2012)1091-1096.

Highlights

- A series of novel purine- pyridone derivatives have been designed and synthesized.
- SKLB0533 showed significant antiproliferative activities.
- SKLB0533 effectively inhibited tubulin polymerization.
- SKLB0533 exhibited no activity against 420 kinases and EZH2.
- SKLB0533 exhibited potent antitumor efficacy in the HCT116 xenograft model.